Title
Monitoring multicomponent transport using in situ ATR FTIR spectroscopy

Authors
Beckingham, Bryan S
Lynd, Nathaniel A
Miller, Daniel J

Publication Date
2018-03-01

DOI
10.1016/j.memsci.2017.12.072

Peer reviewed

Monitoring Multicomponent Transport using *In Situ* ATR FTIR Spectroscopy

Bryan S. Beckingham[a,b], Nathaniel A. Lynd[a,c], Daniel J. Miller[a*]

*Corresponding Author: Tel: +1 (510) 495-2353

E-mail Address: danieljmiller@lbl.gov (D. J. Miller)

[a]Joint Center for Artificial Photosynthesis, Chemical Sciences Division, Lawrence Berkeley National Laboratory, Berkeley, CA 94720, United States

[b]Department of Chemical Engineering, Auburn University, Auburn, AL 36849, United States

[c]McKetta Department of Chemical Engineering, University of Texas at Austin, Austin, TX 78712, United States

Abstract

Membranes are a critical component of many energy generation and storage technologies, including artificial photosynthesis systems that reduce atmospheric CO_2 to high-value products. In this study, we used *in situ* ATR FTIR spectroscopy to monitor the crossover of three commonly-reported CO_2 reduction products—methanol, sodium formate and sodium acetate—through Nafion® 117, a common cation exchange membrane. Measurement errors for the permeation of mixtures of solutes are discussed. Permeabilities from one-, two-, and three-solute mixed solutions were measured using a standard diffusion cell, and ATR FTIR spectra were used to obtain time-resolved concentration data that were fit to a model describing transport of ions and small molecules through hydrated polymer films. The permeability of Nafion® 117 to methanol measured using this methodology was in agreement with literature reports. The sorption of methanol, sodium formate, and sodium acetate, and mixtures thereof, were measured

using a desorption technique. From the measured permeabilities and solubilities, diffusivities of each solute were calculated. Differences in permeability among the solutes were found to be primarily due to differences in their solubility in Nafion® 117.

Keywords

Permeability, multicomponent transport, artificial photosynthesis, *in situ* ATR FTIR spectroscopy

1. Introduction

Permselective membranes are an integral component of many energy generation and storage devices, including fuel cells, electrolyzers, and solar fuels devices. These electrochemical devices typically use two electrodes to carry out the required oxidation and reduction reactions. Membranes in these devices separate the two electrodes, and are responsible for permitting the selective transport of ions between electrodes to maintain overall charge neutrality, but limiting the transport of the oxidation and reduction products produced at the electrodes [1,2]. Therefore, the development of tools for characterizing the transport of ions and neutral molecules through these membranes is vital, as evidenced by the numerous reports of methanol crossover through ion exchange membranes that have emerged from the direct methanol fuel cell community [3–7].

Recently, concerns regarding the availability of fossil fuels and the impact of CO_2 emissions on the global climate have driven the development of technologies for the reduction of CO_2 to high-value products, including transportation fuels [8,9]. Artificial photosynthesis of hydrocarbons from CO_2 uses captured solar energy to drive the oxidation of water and the reduction of CO_2 [2,10,11]. One of the major challenges in the development of artificial photosynthesis devices is a lack of CO_2 reduction catalyst selectivity [11]. Metallic catalysts, such as copper and copper alloys, typically do not reduce CO_2 to a single product, but produce a multiplicity of products, including gases (*e.g.*, carbon monoxide, methane, ethylene), alcohols (*e.g.*, methanol, ethanol, propanol), and charged organic species (*e.g.*, formate and acetate) [9,11]. Therefore, membranes employed in artificial photosynthesis devices must be able to simultaneously limit the transport of multiple CO_2 reduction products in aqueous electrolyte.

Solute transport through dense, hydrated polymer membranes is described by the well-known solution-diffusion model [12]:

$$\langle P_i \rangle = K_i \langle \acute{D}_i \rangle \quad (1)$$

where $\langle P_i \rangle$ is the apparent permeability of the membrane to component *i*, K_i is the solubility of component *i* in the membrane, and $\langle \acute{D}_i \rangle$ is the apparent diffusivity of component *i* in the membrane [13]. The diffusivity describes the movement of a solute through the membrane polymer matrix, and the solubility describes the thermodynamic partitioning of a solute from an external solution into the polymer [14,15].

In the case of a mixture of solutes, the presence of a solute in a membrane may affect the diffusion and/or sorption of other solutes. Coupled fluxes in electrolytic systems have been shown to affect the diffusion of solutes in three-solute mixed solutions through polyamide membranes [16]. Electrostatic interactions among multiple solutes, especially in mixtures of non-ideal, highly polar solutes (*e.g.*, many electrolytes), can contribute to unexpected fluxes. Strong coupling of fluxes among solutes can reduce the selectivity of the membrane, since solutes that might ordinarily be rejected are transported through the membrane with a co-solute [16]. The transport of ion mixtures has also been shown to differ considerably from the transport of a single ion pair. For example, in sulfonated polymers, monovalent ion transport increases in the presence of divalent ions [17,18]. The mechanisms responsible for this behavior are not presently well understood. Multicomponent transport effects have also been reported in the gas separation literature, where competitive sorption phenomena often influence the transport of gas mixtures through polymeric membranes [19]. When multiple solutes are present, the permeabilities of one or more solutes tend to decrease relative to the permeabilities exhibited by each individual solute [19]. Phenomena such as flux coupling and competitive sorption make prediction of multicomponent transport from single component data challenging, and highlights the importance of direct measurement of multicomponent transport parameters [20].

The measurement of small molecule and ion transport through hydrated polymer films is often made using a diffusion cell [21–23]. The hydrated membrane is clamped between a donor chamber (containing a solution at relatively high concentration) and a receiver chamber (containing a solution at relatively low concentration). Due to the gradient in solute chemical potential between the donor chamber and the receiver chamber, the solute of interest diffuses from the donor chamber, through the membrane, and into the receiver chamber. The permeability of the membrane may be calculated from time-resolved receiver chamber concentration data. However, techniques to measure the receiver chamber concentration, such as conductivity (in the case of ion transport experiments [21,22]), are often incapable of discriminating among different solutes, making the measurement of multicomponent transport difficult. Techniques that can discriminate among solutes, such as gas chromatography or mass spectrometry, require periodic aliquot sampling [3], which is labor intensive and complicates the calculation of membrane permeability because the receiver chamber volume decreases with each aliquot removed.

In light of these limitations, we developed a method of measuring multicomponent transport through a hydrated membrane in a standard diffusion cell using continuous *in situ* attenuated total reflectance Fourier transform infrared (ATR FTIR) spectroscopy. Previously, Hallinan and Elabd measured methanol permeability in Nafion® 117 by circulating the receiver chamber solution to a standard benchtop FTIR spectrometer equipped with an ATR cell [5,24–26]. Rather than recirculating the receiver chamber solution to an FTIR instrument [5], an *in situ* ATR FTIR probe can be inserted directly into the receiver chamber and the infrared absorbance continuously measured. For multicomponent permeation experiments, the concentration of each solute in the receiver chamber was measured by deconvolution of infrared absorbance spectra to

extract the relative contributions of each solute. The membrane permeability was then calculated by fitting time-resolved concentration data to a free volume model for ion and small molecule transport in hydrated films [21–23,27,28]. We have previously reported the use of this technique to measure the transport of alcohols, including mixtures of alcohols, in a commercial anion exchange membrane [29]. The methodology presented here is broadly applicable to the measurement of solute permeation through polymer membranes of any type and only requires that the solute of interest have measureable infrared absorption within the detection region of the ATR FTIR spectrometer. In this report, we examine the permeation of mixtures of other CO_2 reduction products, including charged species, in a cation exchange membrane. Methanol, sodium formate, and sodium acetate are three reported products of CO_2 reduction by a copper electrocatalyst [11]. The permeability of Nafion® 117, a widely-used cation exchange membrane [3] that has already seen application in solar fuels devices [30–32], to these three reduction products was measured. (Generally, solar fuels devices do not require the high current densities that might inspire the use of thinner membranes in other electrochemical devices [1].) The permeability of Nafion® 117 to methanol has been reported elsewhere, such as in the fuel cell literature, making it a useful proof-of concept membrane for this study [3]. The permeability to methanol, sodium formate, and sodium acetate alone as well as in two- and three-solute mixtures was measured. The solubility of each solute (alone and in mixtures) in Nafion® 117 was measured using a previously-reported desorption technique [15]. From the measured solubilities and permeabilities, solute diffusivities were calculated. This technique permits quantitative measurement of the simultaneous permeation of multiple solutes with infrared absorbance through hydrated membranes.

2. Experimental Methods

2.1 Materials

Methanol, sodium formate, and sodium acetate (reagent grade, ≥ 99.0% purity) were used as received from Sigma-Aldrich (St. Louis, MO). Ultrapure water was obtained from an EMD Millipore Milli-Q Integral 3 water purification system (18.2 MΩ•cm at 25 °C, 1.2 ppb TOC) (Billerica, MA). Nafion® 117 was obtained from the Fuel Cell Store (College Station, TX) and cut into 35 mm diameter circles using a hammer-driven steel hole punch. Each membrane sample was hydrated in ultrapure water for at least 72 hours prior to use.

2.2 Preparation of one-, two-, and three-solute solutions

Solutions were prepared in 50 mL volumetric flasks. The requisite quantities of methanol, sodium formate and/or sodium acetate were metered into the volumetric flask by weight followed by a small amount of ultrapure water (*ca*. 20 mL). The flask was then swirled to form a homogeneous solution before adding the remaining ultrapure water to achieve the desired 50 mL volume.

2.3 In situ ATR FTIR spectroscopy of calibration solutions

Solutions were prepared over a range of concentrations from 0.01–1.0 M in methanol, sodium formate, and/or sodium acetate in ultrapure water. *In situ* ATR FTIR spectroscopy was conducted using a Mettler-Toledo ReactIR™ 15 outfitted with a shallow tip 9.5 mm DSub AgX DiComp probe. Spectra consisting of 256 averaged scans were obtained over the range 650 cm^{-1} to 2500 cm^{-1} for each solution. A typical experiment consisted of collecting an ultrapure water spectrum to serve as the spectral background. The *in situ* ATR FTIR probe was completely dried

and then immersed in a solution of methanol, sodium formate, and/or sodium acetate and at least four spectra were collected. Lastly, the probe was thoroughly rinsed with ultrapure water and spectra of ultrapure water were again obtained to ensure probe cleanliness for subsequent measurements. The ultrapure water spectrum was subtracted from each solution spectrum, and each solution spectrum was baseline corrected such that the total absorbance was fixed to a value of zero at 1067 cm^{-1}, where no absorbance was exhibited by methanol, sodium formate, or sodium acetate.

2.4 Permeation experiments

All permeation experiments utilized solutions that were 1.0 M in methanol, sodium formate, or sodium acetate, or mixtures thereof in ultrapure water. Solutions were prepared analogously to those used for calibrations. Permeability measurements were conducted in a standard diffusion cell (Adams and Chittenden Scientific Glass, Berkeley, CA). Each half cell had a 3/8” sampling port on the top and a 15 mm diameter orifice in a vertical ground glass face. Both halves of the diffusion cell were jacketed and water from a recirculating heater was used to maintain the diffusion cell temperature at 25 °C. The hydrated membrane was sandwiched between two thin silicone gaskets (35 mm overall diameter with a 15 mm orifice in the center) to prevent leaks. The membrane and gaskets were then clamped between halves of the diffusion cell. The receiver chamber was initially charged with 30 mL of ultrapure water and the *in situ* ATR FTIR probe was inserted into the sampling port, ensuring that the probe tip was fully wetted. Details of the experimental setup, including a photograph of the diffusion cell apparatus, can be found elsewhere [29].

An ultrapure water spectrum was collected to serve as the spectral background. The donor chamber was charged with 30 mL of the donor solution. ATR FTIR spectra were collected over the range 650 cm^{-1} to 2500 cm^{-1} at one minute intervals for approximately 24 hours, which ensured that the receiver chamber solution concentration was always at least an order of magnitude lower than that of the donor chamber solution (*i.e.*, ≤ 0.1 M). The ultrapure water spectrum was subtracted from each spectrum, and each spectrum was baseline corrected such that the total absorbance was fixed to a value of zero at 1067 cm^{-1}, where no absorbance was exhibited by methanol, sodium formate, or sodium acetate. After the permeation experiment was completed, the film thickness was measured using a digital caliper.

2.5 Osmotic flow experiments

During a permeation experiment, water tended to flow from the receiver chamber to the donor chamber due to the osmotic pressure of the solution in the donor chamber. The direction of this flow was, therefore, against that of the methanol, sodium formate, and/or sodium acetate, and would affect the apparent diffusivity calculated for each solute. A modified diffusion cell apparatus, shown in Figure S1 of the Supporting Information, was used to measure the osmotic water flow. A fully hydrated Nafion® 117 membrane was sandwiched between silicone gaskets and mounted between the chambers. One chamber was filled with ultrapure water, and the other chamber was filled with a solution that was 1.0M in methanol, sodium formate, or sodium acetate, or mixtures thereof in ultrapure water. Both halves of the diffusion cell were jacketed and water from a recirculating heater was used to maintain the diffusion cell temperature at 25 °C. Each chamber was carefully filled to assure that no air bubbles were present inside either chamber. The fluid volume change on each side of the membrane was recorded as a function of

time over the course of approximately 30 minutes. This short experimental duration ensured that there was very little concentration change in either chamber, and was sufficient to observe a linear change in volume with time (suggesting that the osmotic flow was pseudo-steady state). The mass flux of water was calculated using the density of water, the cross-sectional area available for water transport through the membrane, and the membrane thickness (measured after the experiment).

2.6 Solubility experiments

The solubility of methanol, sodium formate, and sodium acetate in Nafion® 117 was measured using a desorption technique [15]. Membrane films were fully hydrated in ultrapure water for at least 72 hours prior to measurement. Films were removed from the water, quickly blotted dry, and transferred to a jar containing *ca*. 30 mL of solute solutions (1.0 M in methanol, sodium formate, or sodium acetate, and mixtures thereof), and soaked for 72 hours. Films were removed from their soaking solutions, quickly blotted dry, and the diameter and thickness of each film were recorded. Films were quickly transferred to a clean jar containing a precisely known volume of ultrapure water (*ca.* 15 mL). After soaking 72 hours, solute concentration in the desorption solution was measured using a Thermo Fisher (Waltham, MA) Ultimate 3000 UHPLC system outfitted with a VWD-3100 Variable Wavelength UV detector and an ERC RefractoMax 520 refractive index detector. To ensure that all of the solute had desorbed, films were placed in a new jar containing a precisely know volume of ultrapure water (*ca*. 15 mL) and soaked for an additional 72 hours. No solutes were detected following this second soak in ultrapure water, suggesting that all of the solute desorbed in the first soaking solution. The solubility of each solute in the polymer was calculated as [15]:

$$K_i = \frac{c_i^m}{c_i^s} \tag{2}$$

where c_i^m is the concentration of solute *i* in the membrane and c_i^s is the concentration of solute *i* in the external solution (1.0 M). The concentration of solute in the membrane c_i^m can be calculated from the measured concentration of solute in the desorption solution, the desorption solution volume, and the volume of the swollen membrane sample. After fully desorbing the solutes, the membranes were dried in a vacuum oven for several days until a constant mass was recorded.

3. Results and Discussion

3.1 Determination of effective molar absorptivites

The Beer-Lambert Law relates the absorption of light by an analyte as it passes through a solution to the concentration of the analyte [33]:

$$A_\lambda = \log\left(\frac{I_0}{I}\right) = E_\lambda lc \tag{3}$$

where A_λ and E_λ are the measured absorbance and the molar absorptivity at wavenumber λ, respectively, I_o and I are the incident and transmitted intensity of the light, respectively, c is the solution concentration, and l is the path length the incident light travels through the solution. Here, the transmission distance is identical for each measurement; therefore, an effective molar absorptivity ε_λ, where $\varepsilon_\lambda = E_\lambda l$, is used yielding a single-parameter linear dependence of absorbance on solution concentration:

$$A_\lambda = \varepsilon_\lambda c \tag{4}$$

The concentration of a single component solution can be determined using the measured absorbance from the ATR FTIR spectra—such as those shown in Figure 1 for 1.0 M solutions of methanol, sodium formate, and sodium acetate—at any wavenumber where appreciable absorbance is observed using the effective molar absorptivity. In each of these spectra, the absorbance of ultrapure water has been subtracted; therefore, the absorbances shown in Figure 1 are attributable only to methanol, sodium formate, and sodium acetate.

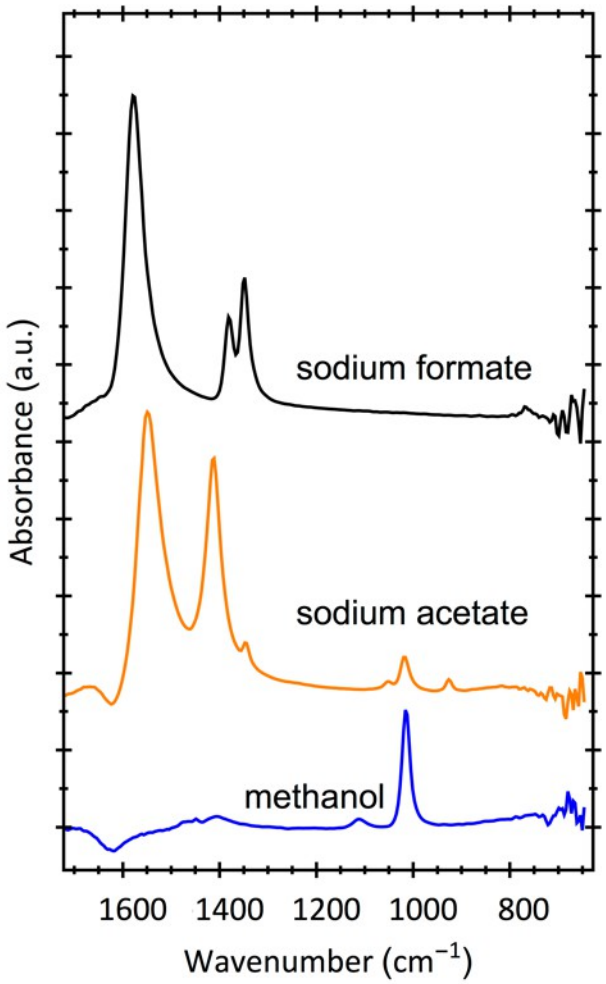

Figure 1. ATR FTIR spectra of 1.0 M solutions of (—) sodium formate, (—) sodium acetate, and (—) methanol between 650 cm^{-1} and 1700 cm^{-1}. Spectra are offset for clarity.

To develop calibration curves from which effective molar absorptivities may be calculated, a series of standard solutions of methanol, sodium formate, and sodium acetate with

concentrations ranging from 0.01 M to 1.0 M were prepared and their ATR FTIR spectra were obtained, as shown for methanol in Figure 2. The practical lower limit for concentration measurement with the *in situ* ATR FTIR instrument was 0.01 M; at lower concentrations, absorbance data were found to have limited reliability.

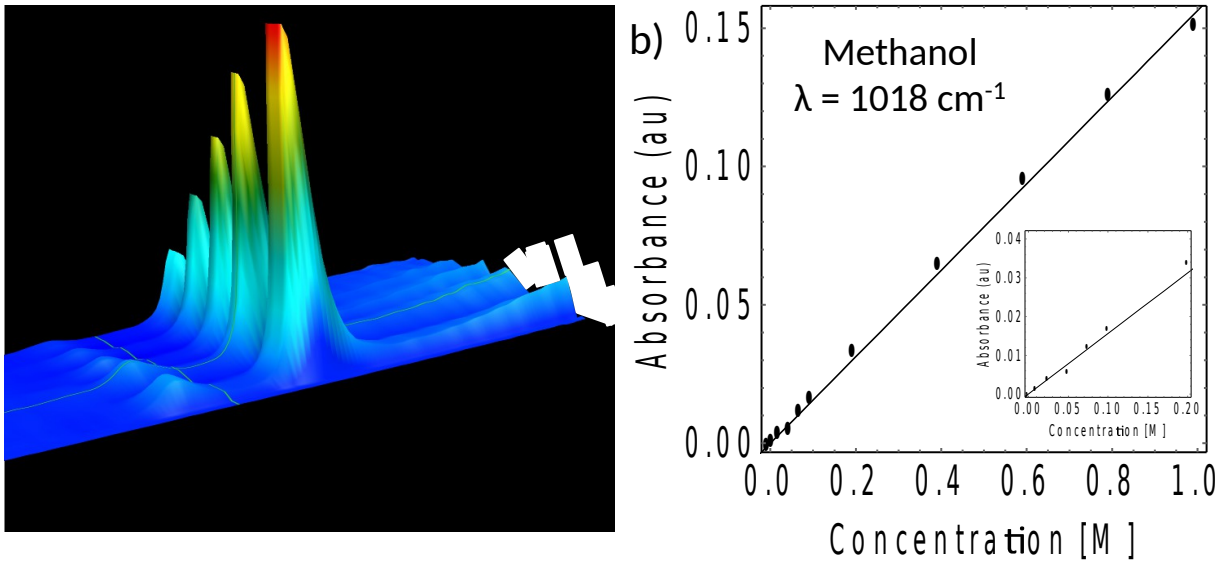

Figure 2. a) ATR FTIR spectra of methanol at increasing concentrations and b) the linear least-squares fitting of the absorbance versus concentration data at 1018 cm^{-1}. The error bars in this figure are smaller than the symbols.

Absorbance was measured at several wavenumbers, chosen based on the spectra shown in Figure 1. The effective molar absorptivity of each solute at each chosen wavenumber was determined by linear least-squares regression fit to the obtained absorbance data, as shown in Figure 3. Insets show calibration data obtained over the range of 0 – 0.1 M, the typical concentration range measured in the receiver chamber during permeation experiments. Note that the effective molar absorptivities were obtained for all three solutes at the wavenumbers of interest for all three solutes, even if no substantial absorption band is apparent for that solute (*e.g.*, sodium formate at 1115 cm^{-1}, *c.f.* Figure 1). At wavenumbers where water has strong absorption bands, increasing solute concentration can lead to a reduction in the water background resulting in small negative effective molar absorptivities (*e.g.*, methanol at 1581 cm^{-1}, *c.f.* Figure 3a) in the background-subtracted spectra. Such strong absorption by water is typically due to O-H-O "scissors" bending [34]. (This phenomenon is also responsible for the apparently negative peak at 1635 cm^{-1}in the methanol spectrum shown in Figure 1.) Overall, excellent linear calibration curves with typical squared correlation coefficients (R^2) values greater than 0.99 were obtained, from which the effective molar absorptivities were calculated (see Table S1 in the Supporting Information for a compilation of all determined effective molar absorptivities and the associated squared correlation coefficients for linear fits to concentration data) for each solute. The wavenumbers where concentration data exhibited both high effective molar absorptivities and high squared correlation coefficients were at 1018 cm^{-1} for methanol (ε = 0.1563, R^2 = 0.9981), 1346 cm^{-1} for sodium formate (ε = 0.1498, R^2 = 0.9998), and 1413 cm^{-1} for sodium acetate (ε = 0.2938, R^2 = 0.9999).

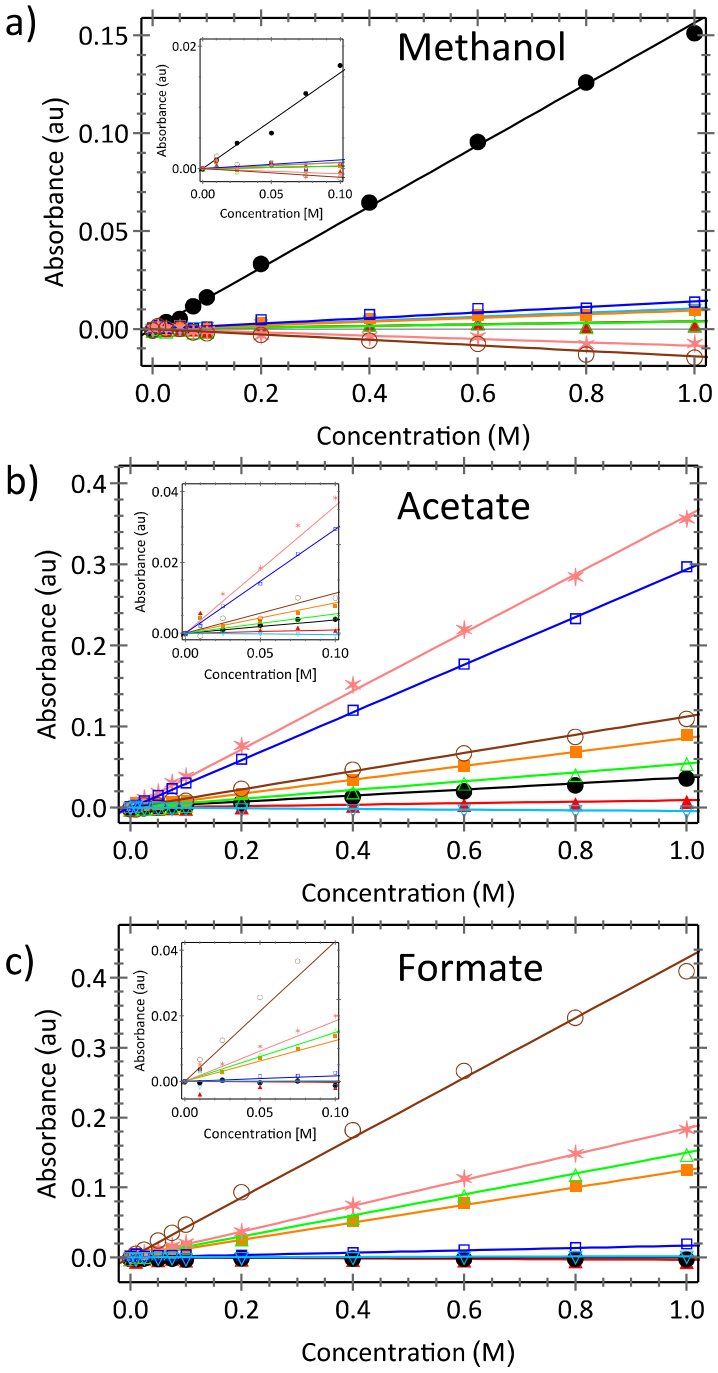

Figure 3. ATR FTIR absorbance plotted against concentration (M) in ultrapure water for a) methanol, b) sodium acetate, and c) sodium formate at various wavenumbers (□) 929 cm^{-1}, (□) 1018 cm^{-1}, (□) 1115 cm^{-1}, (□) 1346 cm^{-1}, (□) 1384 cm^{-1}, (□) 1413 cm^{-1}, (□) 1551 cm^{-1}, and (□) 1581 cm^{-1}. Lines denote linear best-fits to the data. The error bars in this figure are smaller than the symbols.

3.2 Validation of measurement technique with two- and three-solute mixed solutions

For multicomponent solutions, the total infrared absorbance A_j at any wavenumber j is described by a summation of the contributions of each solute i:

$$A_j = \sum_{i=1}^{n} \varepsilon_{ij} c_i \tag{5}$$

As noted in section 3.1, the water background is subtracted from each absorbance measurement. Therefore, while the water solvent may be considered a component of each solution, we are interested only in calculating the concentration(s) of the methanol, sodium formate, and sodium acetate solutes. Determination of the concentrations of n solutes in a mixture using the water-subtracted absorbance of that mixture thereby requires solving a system of n independent equations. For example, to determine the concentrations c_A and c_B in a solution of two solutes A and B, the expansion of Equation (5) yields:

$$\left.\begin{aligned} A_1 &= \varepsilon_{A1} c_A + \varepsilon_{B1} c_B \\ A_2 &= \varepsilon_{A2} c_A + \varepsilon_{B2} c_B \end{aligned}\right\} \tag{6}$$

This system of two equations can be solved for the unknown concentrations c_A and c_B using the absorbances A_1 and A_2 observed at wavenumbers *1* and *2*, and the effective molar absorptivities of solutes A and B at those wavenumbers. An analogous system of three equations can be written for a solution of three solutes A, B, and C:

$$\left.\begin{aligned} A_1 &= \varepsilon_{A1} c_A + \varepsilon_{B1} c_B + \varepsilon_{C1} c_C \\ A_2 &= \varepsilon_{A2} c_A + \varepsilon_{B2} c_B + \varepsilon_{C2} c_C \\ A_3 &= \varepsilon_{A3} c_A + \varepsilon_{B3} c_B + \varepsilon_{C3} c_C \end{aligned}\right\} \tag{7}$$

To examine the utility of the effective molar absorptivities obtained from the one-solute solutions in determining concentrations in multicomponent solute mixtures, a series of two- and three-solute solutions were carefully prepared with individual solute concentrations ranging from

0.05 M to 0.75 M. For each combination of methanol, sodium formate, and sodium acetate, four equimolar solutions were prepared where each component had a concentration of 0.05 M, 0.25 M, 0.50 M, and 0.75 M. Additionally, two non-equimolar solutions were prepared for each solute combination, with one component at 0.25 M and the other at 0.75 M. The absorbance of each of these solutions was measured and concentrations calculated as described above. The calculated concentrations were compared to the actual solution concentrations. The capability of the *in situ* ATR FTIR instrument to accurately determine solute concentration is a function of instrument sensitivity, solute concentration, and solute molar absorptivity. For the present instrument and solute system of methanol, sodium formate, and sodium acetate, agreement between the actual and calculated concentrations was generally excellent, with nearly all solutes exhibiting less than 10% error in the calculated concentration at each measured concentration, and most exhibiting less than 5% deviation from the actual concentration. A detailed description of validation experiments using two- and three-solute mixed solutions is given in the Supporting Information. However, for each new solute or combination of solutes, the experimentalist is encouraged to perform a similar error analysis to empirically assess the accuracy of measured solute concentrations. As noted in section 3.1, the choice of wavenumbers where each solute has a relatively high molar absorptivity will likely result in more accurate concentration measurements than wavenumbers where a solute exhibits relatively low molar absorptivity, as is borne out in Tables S2-S6 in the Supporting Information. When performing permeability experiments, as described in the next section, it is important that the experimentalist be cognizant of instrument sensitivity, and to only make use of absorbance data corresponding to concentrations higher than the practical lower limit of concentration measurement (for the present system, approximately 0.01 M).

3.3 Permeability experiments

The close agreement between measured and actual solute concentrations in two- and three-solute solutions described in the preceding section demonstrates that *in situ* ATR FTIR can be used to quantitatively measure solute concentrations in multicomponent mixtures. Next, we used this technique to monitor the evolution of solute concentration in the receiver chamber of a standard diffusion cell during membrane permeation experiments. The absorbance of the receiver chamber solution was sampled at one minute intervals over a period of approximately 24 hours. Exemplary time-resolved absorbance data at several wavenumbers in the receiver chamber for co-permeation of methanol, sodium formate, and sodium acetate from a mixed donor solution, is shown in Figure 4. From such absorbance data, the concentration of methanol, sodium formate, or sodium acetate was calculated using Equation (4) for single solute permeation experiments. For two- or three-solute co-permeation experiments, a system of two or three equations based on Equation (5) was written (*i.e.*, Equation (6) or (7)) and solved simultaneously for the concentrations of the solutes for each absorbance measurement.

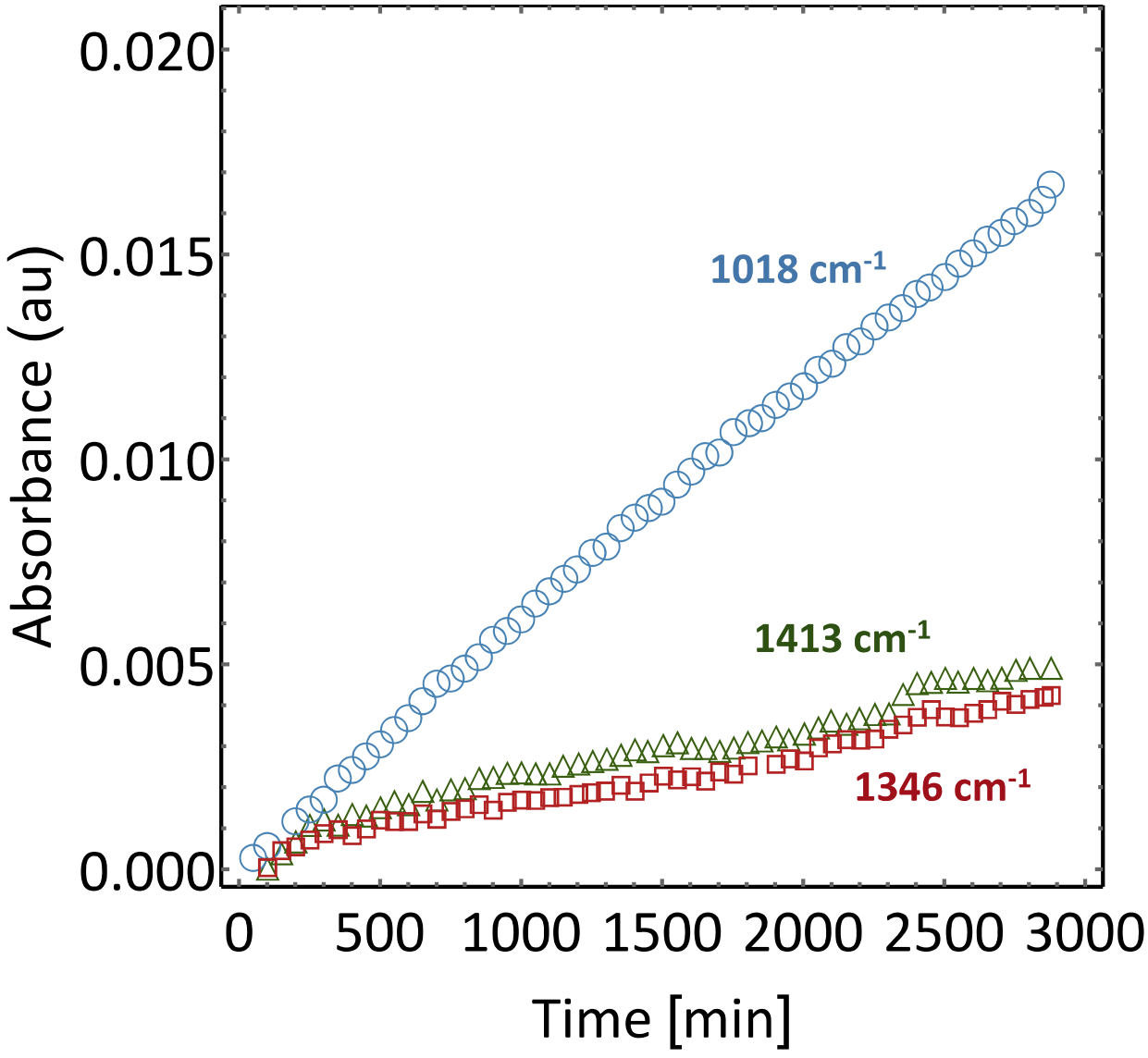

Figure 4. Exemplary time-resolved receiver chamber absorbance data for the co-permeation of methanol, sodium formate, and sodium acetate from a mixed donor solution through Nafion® 117. The absorbances at 1018, 1346, and 1413 cm^{-1} after subtracting the absorbance due to the water background are shown.

Concentration data were fit to a model developed by Yasuda *et al.* that describes the transport of ions and small molecules through hydrated, dense polymer films. The apparent permeability, $\langle P_i \rangle$, of the membrane to solute i was calculated according to Equation (8) [27,28]:

$$\ln\left(1-2\frac{c_{it}}{c_{i0}}\right)=\langle P_i\rangle\left(\frac{-2A}{Vl}t\right) \tag{8}$$

where c_{it} is the concentration of solute i at time t, c_{i0} is the initial concentration of solute i in the donor chamber (1.0 M), A is the membrane cross-sectional area available for transport (1.767 cm^2), V is the volume of the donor and receiver chambers (30 mL), and l is the membrane thickness. The membrane thickness was always measured after the permeation experiment because osmotic de-swelling, which is the transport of water out of the membrane due to the presence of salts in a solution with which the membrane is in contact, can lead to a reduction in membrane thickness relative to the membrane thickness measured after swelling in ultrapure water only [21]. Figure 5 shows the calculated concentrations of methanol, sodium formate, and sodium acetate in the receiver chamber for a permeability experiment with a three-solute mixed solution in the donor chamber. Figure 5 also shows fits of the Yasuda model to time-resolved concentration data.

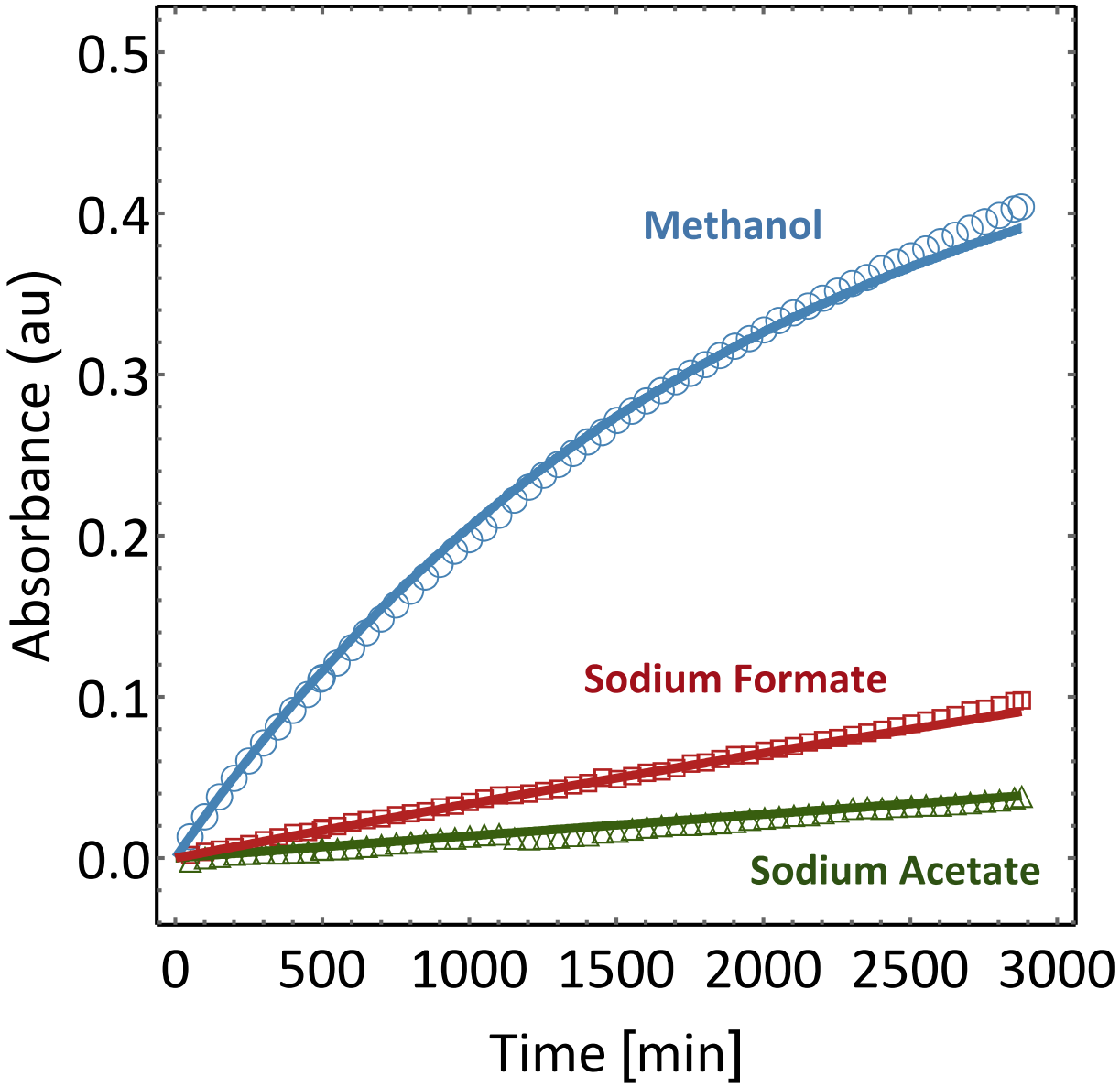

Figure 5. Receiver chamber concentration of methanol, sodium formate, and sodium acetate in a co-permeation experiment from a mixed solution of 1M methanol, 1M sodium formate, and 1M sodium acetate in the donor chamber. Lines are fits of the Yasuda model to concentration data. The concentration of each solute was calculated once per minute; for clarity, only 5% of concentration data are shown.

3.3.1 Permeability of Nafion® 117 to methanol, sodium formate, and sodium acetate

Calculated apparent diffusive permeabilities of Nafion® 117 to methanol, sodium formate, and sodium acetate are shown in Table 1. The apparent permeabilities to methanol, sodium formate, and sodium acetate alone are shown in the first row. Many reports of methanol

crossover through Nafion® 117 are found in the fuel cell literature, so this membrane/solute pair served as a useful benchmark system for this proof-of-concept study. Reported permeabilities of Nafion® 117 to methanol vary due to, among other factors, pretreatment method and measurement technique [35]. The apparent permeability of Nafion® 117 to methanol observed here (1.56×10^{-6} cm^2/s) is in agreement with several literature reports [3,5,24,36,37], suggesting that *in situ* ATR FTIR spectroscopy is an accurate means of tracking concentration during permeation experiments in a standard diffusion cell. The apparent permeability to methanol was about an order of magnitude higher than the apparent permeability to sodium formate, and the permeability to sodium formate was about twice the permeability to sodium acetate.

The apparent permeabilities to methanol, sodium formate, and sodium acetate when co-permeating from two- and three-solute mixed solutions are also shown in Table 1. Generally, the apparent permeabilities to sodium formate and sodium acetate were one to two orders of magnitude lower than the apparent permeability to methanol in two-solute mixtures. The apparent permeability to methanol was lower when co-permeating with sodium formate, sodium acetate, or both than when permeating alone. The apparent permeabilities to sodium formate and sodium acetate were higher when co-permeating from two- or three-solute mixtures than when permeating alone. The apparent permeability to methanol from a three-solute mixed solution was an order of magnitude higher than that of sodium formate from a three-solute mixed solution, and the apparent permeability to sodium formate was about twice that to sodium acetate from three-solute mixed solution.

Table 1. Apparent diffusive permeabilities of methanol, sodium formate, sodium acetate, and mixtures thereof in Nafion® 117. For three-solute mixtures, co-solutes were: (a) sodium formate and sodium acetate, (b) methanol and sodium acetate, (c) methanol and sodium formate. Uncertainties are standard deviations on three replicate measurements.

Apparent Solute Diffusive Permeabilities (cm^2/s) in Nafion® 117			
	Methanol	**Sodium Formate**	**Sodium Acetate**
Single Solute	$(1.56 \pm 0.09) \times 10^{-6}$	$(9.4 \pm 0.9) \times 10^{-8}$	$(5.0 \pm 0.4) \times 10^{-8}$
Two-solute Mixture with Methanol	--	$(1.0 \pm 0.1) \times 10^{-7}$	$(6 \pm 1) \times 10^{-8}$
Two-solute Mixture with Sodium Formate	$(1.1 \pm 0.2) \times 10^{-6}$	--	$(8 \pm 1) \times 10^{-8}$
Two-solute Mixture with Sodium Acetate	$(1.1 \pm 0.1) \times 10^{-6}$	$(1.5 \pm 0.1) \times 10^{-7}$	--
Three-solute Mixture	$(1.0 \pm 0.1) \times 10^{-6(a)}$	$(1.8 \pm 0.7) \times 10^{-7(b)}$	$(8 \pm 4) \times 10^{-8(c)}$

3.3.2 Solubility of methanol, sodium formate, and sodium acetate in Nafion® 117

Transport in dense, hydrated membranes like Nafion® is described by the solution-diffusion model (Equation (1)) [36]. Characterization of solute solubility and diffusivity could give insight pertaining to the underlying phenomena governing overall observed permeabilities. The solubilities of methanol, sodium formate, and sodium acetate in Nafion® 117 are shown in Table 2. Reported values for the partitioning of methanol from solution into Nafion® 117 vary over the range 0.4-1.0 [5,38]. Such variability could be the result of different pretreatment protocols or measurement techniques. The solubility of methanol in Nafion® 117 from 1.0 M solution was in reasonable agreement with previously reported values obtained by electrochemical techniques [38]. Generally, the solubilities mirror trends in permeabilities. For single solutes, the solubility of methanol was about an order of magnitude higher than that of sodium formate, and the solubility of sodium formate was about twice that of sodium acetate. Nafion® is a phase-separated cation exchange polymer comprised of a hydrophobic

polytetrafluoroethylene backbone and hydrophilic side chains containing ionic sulfonate moieties [35]. The hydrophilic side chains cluster together, forming ion-rich channels that are highly hydrated and through which the majority of small molecule transport occurs [35]. The negatively-charged sulfonate groups in the hydrated channels of Nafion® create electrostatic repulsion between the polymer matrix and the negatively-charged formate and acetate ions (*i.e.*, Donnan exclusion) [12]. These electrostatic repulsions, and the resultant exclusion of ions from a charged polymer matrix, have been extensively discussed elsewhere [39,40]. Therefore, the solubility of neutral, polar methanol is higher than the solubility of the electrostatically repulsed formate and acetate ions.

Table 2. Solubilities of methanol, sodium formate, sodium acetate, and mixtures thereof in Nafion® 117. For three-solute mixtures, co-solutes are: (a) sodium formate and sodium acetate, (b) methanol and sodium acetate, (c) methanol and sodium formate. Uncertainties are standard deviations on three replicate measurements.

Solute Solubilities in Nafion® 117			
	Methanol	**Sodium Formate**	**Sodium Acetate**
Single Solute	0.482 ± 0.009	0.075 ± 0.005	0.036 ± 0.002
Two-solute Mixture with Methanol	--	0.073 ± 0.001	0.0407 ± 0.0006
Two-solute Mixture with Sodium Formate	0.37 ± 0.01	--	0.050 ± 0.001
Two-solute Mixture with Sodium Acetate	0.36 ± 0.01	0.100 ± 0.002	--
Three-solute Mixture	0.43 ± 0.01[(a)]	0.110 ± 0.001[(b)]	0.061 ± 0.001[(c)]

The sorption of methanol from two- and three-solute mixtures with sodium formate and/or sodium acetate decreased relative to the sorption from a solution of methanol only. This result could be due to a competitive sorption effect [19], where the presence of sodium formate and/or sodium acetate somewhat precluded the sorption of methanol. Relative to the sorption

from a mixed solution of methanol and sodium formate or of methanol and sodium acetate, the sorption of methanol from a mixed solution of methanol, sodium formate, and sodium acetate slightly increased. This result could be due to osmotic de-swelling of the membrane when it was in contact with solutions containing sodium formate and/or sodium acetate. Increases in ion concentration inside a polymer film have previously been attributed to osmotic deswelling in ion sorption experiments [15].

Table 3 shows the swollen volume of membranes equilibrated in various one-, two-, and three-solute solutions relative to the swollen volume of a membrane hydrated in ultrapure water. Measurements of sample film diameters and thicknesses were made in triplicate and standard deviations on the average diameters and thicknesses were calculated. Swollen volumes were calculated from these measured diameter and thickness values, and the uncertainties shown in Table 3 were propagated from the standard deviations on average diameters and thicknesses as described by Harris [41]. Equilibration of Nafion® 117 against a 1.0 M methanol solution induced a negligible increase in swelling relative to that of a membrane equilibrated in ultrapure water. The uptake of methanol is reportedly higher than that of water in Nafion® [35], which could lead to this slight increase in swollen volume. However, both sodium formate and sodium acetate induced appreciable de-swelling of the membrane. When a membrane swollen in pure water is brought into contact with a salt solution, the osmotic pressure of that solution acts to draw water out of the membrane, reducing the volume of the membrane. Within the context of solubility measurements, osmotic de-swelling decreases the sample volume, concentrating the solutes within the membrane and effectively increasing the solubility coefficient (Equation (2)). Indeed, as shown in Table 3, the relative swollen volume of Nafion® 117 was lower when

equilibrated against a three-solute mixed solution of methanol, sodium formate, and sodium acetate than when equilibrated against a two-solute mixed solution of methanol and sodium formate or methanol and sodium acetate. This increased osmotic de-swelling effect was likely due to the higher overall ionic strength of the three-solute solution than the two-solute solution. Therefore, the observed solubility of methanol in Nafion® 117 from a three-solute solution was higher than the solubility of methanol in Nafion® 117 from a two-solute solution. Sorption of solutes from two- and three-solute solutions was likely influenced by both competitive sorption effects and osmotic de-swelling effects.

Table 3. Relative swollen volume of Nafion® 117 membranes equilibrated against ultrapure water as well as one-, two-, and three-solute solutions of methanol, sodium formate, and sodium acetate. All volume measurements were normalized against the volume of a membrane swollen in ultrapure water only. All solutes were at a concentration of 1.0 M. Uncertainties are propagated (as described by Harris [41]) from standard deviations on three replicate measurements of sample film diameters and thicknesses.

Solute(s) in Equilibration Solution	Relative Swollen Volume of Nafion® 117
None (ultrapure water only)	1.00 ± 0.05
Methanol	1.01 ± 0.04
Sodium Formate	0.89 ± 0.03
Sodium Acetate	0.90 ± 0.03
Methanol + Sodium Formate	0.93 ± 0.03
Methanol + Sodium Acetate	0.92 ± 0.04
Sodium Formate + Sodium Acetate	0.89 ± 0.04
Methanol + Sodium Formate + Sodium Acetate	0.89 ± 0.03

The sorption of sodium formate from a mixed solution of methanol and sodium formate was nearly identical to sorption from a solution of only sodium formate (Table 2). Similarly, a slight increase in sodium acetate sorption from a mixed solution of methanol and sodium acetate was observed relative to sorption from a solution of only sodium acetate (Table 2). The presence of methanol within the hydrated channels of the membrane may promote sorption of the sodium formate and sodium acetate. Methanol, a highly polar molecule, may associate with the negatively charged sulfonate side chains on the Nafion® polymer, effectively shielding them and reducing the electrostatic repulsion between the fixed sulfonate charges and the formate and/or acetate anions. Both sodium formate and sodium acetate induce osmotic de-swelling of the membrane, but methanol tends to slightly swell Nafion® (Table 3). Therefore, the relative swollen volume of films equilibrated against a mixed solution of methanol and sodium formate or methanol and sodium acetate lies between the relative swollen volume of films equilibrated against solutions of sodium formate or sodium acetate only and the relative swollen volume of a film equilibrated against ultrapure water only (Table 3). While the swelling induced by the

methanol would tend to dilute the concentration of sodium formate or sodium acetate within the Nafion®, favorable interactions between the methanol and the sulfonate fixed charge groups may promote sodium formate and sodium acetate sorption, resulting in little change from the sorption observed from solutions of sodium formate or sodium acetate only (Table 2).

The sorption of sodium formate and sodium acetate from a mixed solution of sodium formate and sodium acetate was higher than from a mixed solution of methanol and sodium formate or of methanol and sodium acetate (Table 2). The enhanced osmotic de-swelling of the membrane when equilibrated against a mixed solution of sodium formate and sodium acetate resulted in a smaller relative swollen volume (and higher solute concentration inside the membrane) than when equilibrated against a mixed solution of methanol and sodium formate or methanol and sodium acetate (Table 3). The sorption of sodium formate and sodium acetate from a three-solute mixed solution was also higher than sorption from a two-solute mixed solution. The membrane exhibited substantial de-swelling when equilibrated against a three-solute mixed solution (equal to that when equilibrated against a two-solute mixed solution of sodium formate and sodium acetate, or against a solution of only sodium formate or only sodium acetate) (Table 3). However, with the possible electrostatic shielding contribution of methanol from the three-solute mixed solution, the sodium formate and sodium acetate were able to sorb from a three-solute mixed solution to a higher extent than from either one- or two-solute mixed solutions.

3.3.3 Diffusivity of methanol, sodium formate, and sodium acetate in Nafion® 117

From Equation (1), the overall apparent permeability of a polymer to a solute is expressed as the product of the solute solubility and apparent solute diffusivity in the polymer.

Therefore, the apparent diffusivity of methanol, sodium formate, and sodium acetate may be calculated from measured permeabilities (Table 1) and solubilities (Table 2). However, water tends to permeate through the membrane from the receiver chamber to the donor chamber (i.e., in the direction opposite to solute permeation) due to the osmotic pressure of the donor chamber solution. Therefore, the apparent diffusivities of the solutes calculated from the measured permeabilities and solubilities are likely to be lower than the actual diffusivities of the solutes in the hydrated polymer due to the opposing flow (sometimes called convective flow [13,23]) of water through the membrane. Kamcev *et al*. provide a framework that may be used to account for osmotically-induced water flow in the measurement of salt diffusion coefficients [13]. The corrected average diffusivity is given by:

$$\langle D_i \rangle = \frac{\langle P_i \rangle}{K_i}\left(1 - \frac{\omega_i^m}{2}\right) - \frac{P_w d_w (\Delta p - \Delta \pi)\omega_i^m}{2 M_i c_i^m} \tag{9}$$

where ω_i^m is the mass fraction of solute *i* in the membrane at the face in contact with the donor cell solution, P_w is the hydraulic permeability of the membrane, d_w is the density of water, Δp and $\Delta \pi$ are the hydrostatic and osmotic pressure differences between the donor chamber and receiver chamber, M_i is the molecular mass of species *i*, and c_i^m is the concentration of species *i* in the membrane at the face in contact with the donor cell solution. A derivation of this expression can be found elsewhere [13]. The second term on the right side of Equation (9) accounts for the osmotic flow of water across the membrane in the calculation of the corrected diffusivity [13].

The hydraulic permeability is defined as:

$$P_w = \frac{n_w l}{d_w (\Delta p - \Delta \pi)} \tag{10}$$

where n_w is the mass flux of water across the membrane (measured as described in section 2.5). Combination of Equations (9) and (10) yields:

$$\langle D_i \rangle = \frac{\langle P_i \rangle}{K_i}\left(1 - \frac{\omega_i^m}{2}\right) - \frac{n_w l \omega_i^m}{2 M_i c_i^m} \tag{11}$$

Note that the net mass flux of water in the transport experiments described here is in the direction opposite to the net flux of methanol, sodium formate, and/or sodium acetate, so in the calculation of the corrected solute diffusivity (Equation (11)), the second term on the right side is positive. The mass fraction of solute in the membrane at the face in contact with the donor cell solution was calculated by:

$$\omega_i^m = \frac{m_i^m}{m_i^m + m_w^m + m_p} \tag{12}$$

where m_i^m is the mass of solute *i* in the membrane, m_w^m is the mass of water in the membrane, and m_p is the mass of dry polymer. The mass of solute in the membrane was calculated from the number of moles of solute desorbed from the polymer in a solubility experiment and the solute molecular weight. The mass of water in the membrane was calculated as the difference between the hydrated membrane mass and the dry membrane mass.

Table 4 shows the corrected, average diffusivities of methanol, sodium formate, and sodium acetate in Nafion® 117 when diffusing in one-, two- and three-solute mixtures. Uncertainties shown in Table 4 were calculated by propagating standard deviations on average measured values through Equations (9) - (12), as described in Harris [41]. Uncorrected diffusivities, calculated by Equation (1) using only the measured permeabilities (Table 1) and solubilities (Table 2) are listed in Table S8 in the Supporting Information. Examination of the values listed in Tables 4 and S8 reveals that the osmotic flow of water through the membrane had

little impact on the calculated diffusivities, with differences between uncorrected (Table S7) and corrected (Table 4) values lying within experimental uncertainty.

The diffusivity of methanol in Nafion® 117 is in reasonable agreement with previously reported values [5,38]. Generally, all of the diffusivities were similar in magnitude, and do not exhibit the substantial differences among solutes observed for the permeabilities (Table 1) and solubilities (Table 2). Methanol had the highest overall diffusivity when diffusing alone. Sodium formate and sodium acetate had lower diffusivities than methanol, and the diffusivity of sodium acetate was slightly higher than that of sodium formate. The diffusivity of a solute through a polymer is inversely proportional to the size of the solute [42]. The observed trend in diffusivities for methanol, sodium formate, and sodium acetate is consistent with the molecular size of each of these solutes. Methanol is the smallest of the three solutes, with a diameter of 3.6 Å [43], while formate has a diameter of 4.0-4.6 Å [44] and acetate has a diameter of 3.35-4.4 Å [44].

Table 4. Average diffusivities of methanol, sodium formate, sodium acetate, and mixtures thereof in Nafion® 117, corrected for the osmotic flow of water, calculated using Equation (10). For three-solute mixtures, co-solutes are: (a) sodium formate and sodium acetate, (b) methanol and sodium acetate, (c) methanol and sodium formate. Uncertainties are propagated (as described by Harris [41]) from the uncertainties reported for permeabilities and solubilities.

Average Corrected Solute Diffusivities (cm^2/s) in Nafion® 117			
	Methanol	**Sodium Formate**	**Sodium Acetate**
Single Solute	$(3.3 \pm 0.2) \times 10^{-6}$	$(1.4 \pm 0.2) \times 10^{-6}$	$(1.5 \pm 0.1) \times 10^{-6}$
Two-solute Mixture with Methanol	--	$(1.5 \pm 0.2) \times 10^{-6}$	$(1.6 \pm 0.4) \times 10^{-6}$
Two-solute Mixture with Sodium Formate	$(3.3 \pm 0.3) \times 10^{-6}$	--	$(1.9 \pm 0.2) \times 10^{-6}$
Two-solute Mixture with Sodium Acetate	$(3.1 \pm 0.3) \times 10^{-6}$	$(1.7 \pm 0.2) \times 10^{-6}$	--
Three-solute Mixture	$(2.6 \pm 0.2) \times 10^{-6(a)}$	$(1.8 \pm 0.7) \times 10^{-6(b)}$	$(1.5 \pm 0.7) \times 10^{-6(c)}$

Relative to its diffusivity alone, the diffusivity of methanol decreases slightly in two-solute mixtures with sodium formate or sodium acetate, and decreases further in a three-solute mixture with sodium formate and sodium acetate. This trend in decreasing diffusivity follows the trend in swollen volume for Nafion® equilibrated with these solutions. The degree of hydration of a polymer tends to strongly influence the transport of ions and small molecules through the polymer [42]. Diffusion occurs through free volume elements within the polymer matrix, and swelling (caused by sorption of water) tends to increase the fractional free volume of a polymer, leading to higher diffusivities of ions and small molecules in the polymer [42]. As water migrates out of the polymer during osmotic de-swelling (Table 3), the diffusion coefficient of methanol is depressed.

The diffusion coefficients of sodium formate and sodium acetate are, generally, all similar over the various compositions studied here, and are consistent with the relative diameters of the three solutes. These results suggest that the variations in permeability observed among the solutes are likely not strongly tied to variations in diffusivity. Instead, the differences observed in permeabilities are largely correlated with differences in the solubility of the three solutes in Nafion®, and that competitive sorption and osmotic de-swelling effects likely contribute to changes in permeability from two- and three-solute solutions relative to permeability from one-solute solutions.

4. Conclusions

In this study, *in situ* ATR FTIR spectroscopy was used to monitor the transport of methanol, sodium formate, and sodium acetate—three products of electrochemical CO_2 reduction—through Nafion® 117. The concentration of standard solutions of various methanol,

sodium formate, and sodium acetate compositions was accurately measured. The transport of methanol, sodium formate, sodium acetate, and mixtures thereof was monitored using an *in situ* ATR FTIR probe mounted in the receiver chamber of a standard diffusion cell. Permeabilities of Nafion® 117 to methanol, sodium formate, and sodium acetate were extracted using a model developed to describe ion and small molecule transport through hydrated films. The permeability to methanol was about an order of magnitude higher than that of sodium formate, and the permeability to sodium formate was about twice that to sodium acetate. Permeability to methanol decreased in the presence of sodium formate and sodium acetate, while permeability of sodium acetate and sodium formate generally increased in two- and three-solute mixtures. Trends in permeability closely mirrored trends in solute sorption in Nafion® 117, while diffusion coefficients were similar for all three solutes over all compositions, suggesting that differences in permeability among the three solutes were primarily a function of differences in solubility. This study demonstrates that *in situ* ATR FTIR spectroscopy is an effective tool for monitoring concentrations in a standard diffusion cell, and that multicomponent transport may be quantified without the need for periodic aliquot sampling. The transport of solutes with distinct infrared signatures, including many alcohols, ions, and neutral species, could be monitored using this technique, and the permeability of hydrated membrane films to these solutes readily calculated using established models.

Acknowledgements

This material is based upon work performed at the Joint Center for Artificial Photosynthesis, a DOE Energy Innovation Hub, supported through the Office of Science of the U.S. Department of Energy under Award Number DE-SC000493. This work was also supported

by the California Energy Commission (CEC) under contract 500-11-23. BSB gratefully acknowledges start-up funds provided by the Department of Chemical Engineering and the College of Engineering at Auburn University. NAL acknowledges support by the Welch Foundation (Grant No.: F-1904).

References

[1] A. Berger, R.A. Segalman, J. Newman, Material requirements for membrane separators in a water-splitting photoelectrochemical cell, Energy Environ. Sci. 7 (2014) 1468–1476. doi:10.1039/c3ee43807d.

[2] M.R. Singh, E.L. Clark, A.T. Bell, Effects of Electrolyte, Catalyst, and Membrane Composition and Operating Conditions on the Performance of Solar-Driven Electrochemical Reduction of Carbon Dioxide, Phys. Chem. Chem. Phys. 17 (2015) 18924–18936. doi:10.1039/C5CP03283K.

[3] N.W. DeLuca, Y.A. Elabd, Polymer Electrolyte Membranes for the Direct Methanol Fuel Cell: A Review, J. Polym. Sci. Part B Polym. Phys. 44 (2006) 2201–2225. doi:10.1002/polb.20861.

[4] H. Dohle, J. Divisek, J. Mergel, H.F. Oetjen, C. Zingler, D. Stolten, Recent developments of the measurement of the methanol permeation in a direct methanol fuel cell, J. Power Sources. 105 (2002) 274–282. doi:10.1016/S0378-7753(01)00953-3.

[5] D.T. Hallinan, Y.A. Elabd, Diffusion and Sorption of Methanol and Water in Nafion Using Time-Resolved Fourier Transform Infrared−Attenuated Total Reflectance

Spectroscopy, J. Phys. Chem. B. 111 (2007) 13221–13230. doi:10.1021/jp075178n.

[6] A. Heinzel, V.M. Barragán, A review of the state-of-the-art of the methanol crossover in direct methanol fuel cells, J. Power Sources. 84 (1999) 70–74. doi:10.1016/S0378-7753(99)00302-X.

[7] V. Neburchilov, J. Martin, H. Wang, J. Zhang, A review of polymer electrolyte membranes for direct methanol fuel cells, J. Power Sources. 169 (2007) 221–238. doi:10.1016/j.jpowsour.2007.03.044.

[8] M.R. Singh, E.L. Clark, A.T. Bell, Thermodynamic and achievable efficiencies for solar-driven electrochemical reduction of carbon dioxide to transportation fuels, Proc. Natl. Acad. Sci. (2015) 201519212. doi:10.1073/pnas.1519212112.

[9] M.R. Singh, A.T. Bell, Design of an artificial photosynthetic system for production of alcohols in high concentration from CO2, Energy Environ. Sci. 9 (2016) 193–199. doi:10.1039/C5EE02783G.

[10] N.S. Lewis, D.G. Nocera, Powering the planet: chemical challenges in solar energy utilization., Proc. Natl. Acad. Sci. U. S. A. 103 (2006) 15729–35. doi:10.1073/pnas.0603395103.

[11] K.P. Kuhl, E.R. Cave, D.N. Abram, T.F. Jaramillo, New insights into the electrochemical reduction of carbon dioxide on metallic copper surfaces, Energy Environ. Sci. 5 (2012) 7050. doi:10.1039/c2ee21234j.

[12] G.M. Geise, H.-S. Lee, D.J. Miller, B.D. Freeman, J.E. McGrath, D.R. Paul, Water Purification by Membranes: The Role of Polymer Science, J. Polym. Sci. Part B Polym. Phys. 48 (2010) 1685–1718. doi:10.1002/polb.22037.

[13] J. Kamcev, D.R. Paul, G.S. Manning, B.D. Freeman, Accounting for frame of reference

and thermodynamic non-idealities when calculating salt diffusion coefficients in ion exchange membranes, J. Memb. Sci. 537 (2017) 396–406. doi:10.1016/j.memsci.2017.05.034.

[14] G.M. Geise, B.D. Freeman, D.R. Paul, Sodium chloride diffusion in sulfonated polymers for membrane applications, J. Memb. Sci. 427 (2013) 186–196. doi:10.1016/j.memsci.2012.09.029.

[15] G.M. Geise, L.P. Falcon, B.D. Freeman, D.R. Paul, Sodium chloride sorption in sulfonated polymers for membrane applications, J. Memb. Sci. 423–424 (2012) 195–208. doi:10.1016/j.memsci.2012.08.014.

[16] M. Soltanieh, S. Sahebdelfar, Interaction effects in multicomponent separation by reverse osmosis, J. Memb. Sci. 183 (2001) 15–27. doi:10.1016/S0376-7388(00)00554-8.

[17] S.G. Kimura, Reverse Osmosis Performance of Sulfonated Poly(2,6-dimethylphenylene Ether) Ion Exchange Membranes, Ind. Eng. Chem. Prod. Res. Dev. 10 (1971) 335–339. doi:10.1021/i360039a015.

[18] J. Kamcev, B.D. Freeman, Charged Polymer Membranes for Environmental/Energy Applications, Annu. Rev. Chem. Biomol. Eng. 7 (2016) 111–133. doi:10.1146/annurev-chembioeng-080615-033533.

[19] R.T. Chern, W.J. Koros, B. Yui, H.B. Hopfenberg, V.T. Stannett, Selective permeation of CO2 and CH4 through kapton polyimide: Effects of penetrant competition and gas-phase nonideality, J. Polym. Sci. Polym. Phys. Ed. 22 (1984) 1061–1084. doi:10.1002/pol.1984.180220610.

[20] W.J. Koros, R.T. Chern, V. Stannett, H.B. Hopfenberg, A model for permeation of mixed gases and vapors in glassy polymers, J. Polym. Sci. Polym. Phys. Ed. 19 (1981) 1513–

1530. doi:10.1002/pol.1981.180191004.

[21] H. Ju, A.C. Sagle, B.D. Freeman, J.I. Mardel, A.J. Hill, Characterization of sodium chloride and water transport in crosslinked poly(ethylene oxide) hydrogels, J. Memb. Sci. 358 (2010) 131–141. doi:10.1016/j.memsci.2010.04.035.

[22] G.M. Geise, B.D. Freeman, D.R. Paul, Characterization of a sulfonated pentablock copolymer for desalination applications, Polymer. 51 (2010) 5815–5822. doi:10.1016/j.polymer.2010.09.072.

[23] M. Galizia, D.R. Paul, B.D. Freeman, Liquid methanol sorption, diffusion and permeation in charged and uncharged polymers, Polymer. 102 (2016) 281–291. doi:10.1016/j.polymer.2016.09.010.

[24] Y.A. Elabd, E. Napadensky, J.M. Sloan, D.M. Crawford, C.W. Walker, Triblock copolymer ionomer membranes Part I. Methanol and proton transport, J. Memb. Sci. 217 (2003) 227–242. doi:10.1016/s0376-7388(03)00127-3.

[25] Y.A. Elabd, M.G. Baschetti, T.A. Barbari, Time-Resolved Fourier Transform Infrared/Attenuated Total Reflection Spectroscopy for the Measurement of Molecular Diffusion in Polymers, J. Polym. Sci. Part B Polym. Phys. 41 (2003) 2794–2807.

[26] N.W. DeLuca, Y.A. Elabd, Nafion®/poly(vinyl alcohol) blends: Effect of composition and annealing temperature on transport properties, J. Memb. Sci. 282 (2006) 217–224. doi:10.1016/j.memsci.2006.05.025.

[27] H. Yasuda, C.E. Lamaze, L.D. Ikenberry, Permeability of Solutes through Hydrated Polymer Membranes. Part I. Diffusion of Sodium Chloride, Makromol. Chemie. 118 (1968) 19–35. doi:10.1002/macp.1968.021180102.

[28] H. Yasuda, L.D. Ikenberry, C.E. Lamaze, Permeability of Solutes through Hydrated

Polymer Membranes. Part II. Permeability of Water Soluble Organic Solutes, Makromol. Chemie. 125 (1969) 108–118. doi:10.1002/macp.1969.021250111.

[29] B.M. Carter, B.M. Dobyns, B.S. Beckingham, D.J. Miller, Multicomponent transport of alcohols in an anion exchange membrane measured by *in situ* ATR FTIR spectroscopy, Polymer. 123 (2017) 144–152. doi:10.1016/j.polymer.2017.06.070.

[30] J.M. Spurgeon, M.G. Walter, J. Zhou, P.A. Kohl, N.S. Lewis, Electrical conductivity, ionic conductivity, optical absorption, and gas separation properties of ionically conductive polymer membranes embedded with Si microwire arrays, Energy Environ. Sci. 4 (2011) 1772–1780. doi:10.1039/c1ee01028j.

[31] M.R. Singh, J.C. Stevens, A.Z. Weber, Design of Membrane-Encapsulated Wireless Photoelectrochemical Cells for Hydrogen Production, J. Electrochem. Soc. 161 (2014) E3283–E3296. doi:10.1149/2.033408jes.

[32] S. Ardo, S.H. Park, E.L. Warren, N. Lewis, Unassisted solar-driven photoelectrosynthetic HI splitting using membrane-embedded Si microwire arrays, Energy Environ. Sci. 4 (2015) 1166–1169. doi:10.1039/C5EE00227C.

[33] Beer, Bestimmung der Absorption des rothen Lichts in farbigen Flüssigkeiten, Ann. Der Phys. Und Chemie. 162 (1852) 78–88. doi:10.1002/andp.18521620505.

[34] D. Eisenberg, W. Kauzmann, The Structure and Properties of Water, Oxford University Press, New York, NY, 1969.

[35] A. Kusoglu, A.Z. Weber, New Insights into Perfluorinated Sulfonic-Acid Ionomers, Chem. Rev. 117 (2017) 987–1104. doi:10.1021/acs.chemrev.6b00159.

[36] L.A. Diaz, G.C. Abuin, H.R. Corti, Methanol sorption and permeability in Nafion and acid-doped PBI and ABPBI membranes, J. Memb. Sci. 411–412 (2012) 35–44.

doi:10.1016/j.memsci.2012.04.013.

[37] N.W. DeLuca, Y.A. Elabd, Direct methanol fuel cell performance of Nafion®/poly(vinyl alcohol) blend membranes, J. Power Sources. 163 (2006) 386–391. doi:10.1016/j.jpowsour.2006.09.009.

[38] X. Ren, T.E. Springer, T.A. Zawodzinski, S. Gottesfeld, Methanol Transport Through Nation Membranes. Electro-osmotic Drag Effects on Potential Step Measurements, J. Electrochem. Soc. 147 (2000) 466. doi:10.1149/1.1393219.

[39] J. Kamcev, M. Galizia, F.M. Benedetti, E.-S. Jang, D.R. Paul, B.D. Freeman, et al., Partitioning of mobile ions between ion exchange polymers and aqueous salt solutions: importance of counter-ion condensation, Phys. Chem. Chem. Phys. 18 (2016) 6021–6031. doi:10.1039/C5CP06747B.

[40] F.G. Helfferich, Ion Exchange, Dover Publications, New York, NY, 1962.

[41] D.C. Harris, Quantitative Chemical Analysis, Sixth Edit, W. H. Freeman and Company, New York, 2003.

[42] G.M. Geise, D.R. Paul, B.D. Freeman, Fundamental water and salt transport properties of polymeric materials, Prog. Polym. Sci. 39 (2013) 1–42. doi:10.1016/j.progpolymsci.2013.07.001.

[43] H. Wu, Q. Gong, D.H. Olson, J. Li, Commensurate Adsorption of Hydrocarbons and Alcohols in Microporous Metal Organic Frameworks, Chem. Rev. 112 (2012) 836–868. doi:10.1021/cr200216x.

[44] J. Jae, G.A. Tompsett, A.J. Foster, K.D. Hammond, S.M. Auerbach, R.F. Lobo, et al., Investigation into the shape selectivity of zeolite catalysts for biomass conversion, J. Catal. 279 (2011) 257–268. doi:10.1016/j.jcat.2011.01.019.

Supporting Information for Monitoring Multicomponent Transport using *In Situ* ATR FTIR Spectroscopy

Bryan S. Beckingham[1,2], Nathaniel A. Lynd[1,3], Daniel J. Miller[1,*]

*Corresponding Author: Tel: +1 (510)-495-2353

E-mail Address: danieljmiller@lbl.gov (D.J. Miller)

[1]Joint Center for Artificial Photosynthesis, Materials Sciences Division, Lawrence Berkeley National Laboratory, Berkeley, CA 94720, United States

[2]Department of Chemical Engineering, Auburn University, Auburn, AL 36849, United States

[3]McKetta Department of Chemical Engineering, University of Texas at Austin, Austin, TX 78712, United States

1. Measurement of Osmotic Water Flow

The modified diffusion cell apparatus used to measure the flow of water induced by the osmotic pressure of the donor chamber solution is shown in Figure S1.

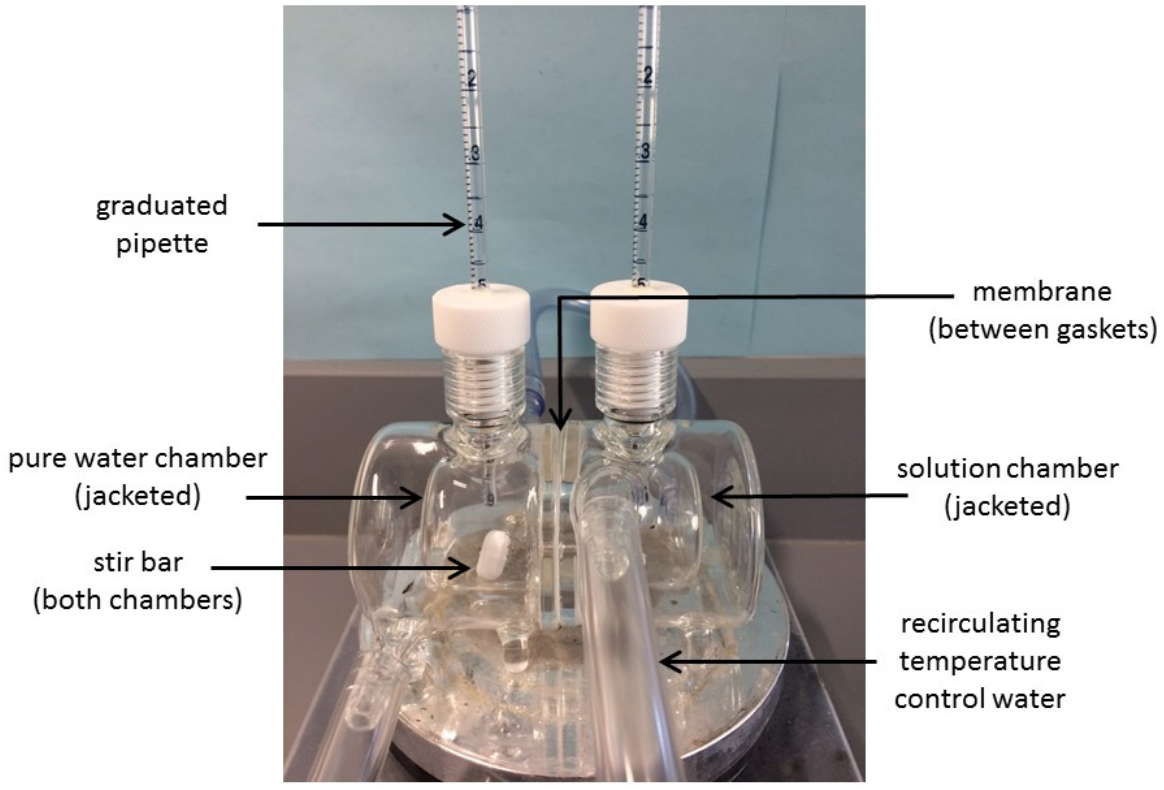

Figure S1. Apparatus used to measure the osmotic flow of water.

The apparatus is essentially the same two-part diffusion cell used for solute permeation experiments [1]. The volume change in each chamber was measured using graduated pipettes. Each pipette was epoxied in a hole drilled in a threaded stopper.

2. Analysis of Single Solute Calibration Solutions

For each of the one-solute solutions, at least four spectra were collected and shifted in baseline absorbance such that $A = 0$ at $\lambda = 1067$ cm^{-1}. Table S1 compiles the effective molar absorptivities (ε_λ) and the squared correlation coefficients (R^2) of their respective fits for a series of wavenumbers of interest for methanol, sodium formate, and sodium acetate.

Table S1: Effective molar absorptivities and their correlation coefficients for 1M methanol, 1M sodium formate, and 1M sodium acetate in aqueous solution.

	Methanol		**Sodium Formate**		**Sodium Acetate**	
λ [cm^{-1}]	ε_λ	R^2	ε_λ	R^2	ε_λ	R^2
928	0.003980	0.74201	-0.003592	0.61024	0.009114	0.83535
1018	0.156278	0.99812	-0.000293	0.01219	0.037327	0.99961
1115	0.010463	0.99829	0.001549	0.45243	-0.004148	0.88979
1384	0.009458	0.97069	0.124837	0.99959	0.085861	0.99851
1346	0.003859	0.73904	0.149816	0.99982	0.054346	0.99610
1413	0.014098	0.97858	0.016715	0.97062	0.293814	0.99991
1551	-0.008539	0.94171	0.184423	0.99970	0.359650	0.99960
1581	-0.013948	0.97579	0.427648	0.99820	0.112431	0.99900

3. Validation of Measurement Method using Two- and Three-solute Mixed Solutions

3.1 Methanol and Sodium Formate

A comparison of actual and measured concentrations (calculated using Equation (6) in the main text) is shown in Figure S2 for mixed solutions of methanol and sodium formate. The most accurate determination of concentrations was realized using the absorbances at 1018 cm^{-1} and 1346 cm^{-1}; concentrations calculated using the absorbances at other wavenumbers can be found in Table S2. Sodium formate exhibits essentially no absorption at 1018 cm^{-1} (Table S1), simplifying the calculation of concentrations for this particular solute pair. A detailed discussion of these calculations is found in the next section of the Supporting Information. The calculated concentrations were in agreement with the actual solution concentrations (evident in their proximity to the identity line), with an average difference between actual and measured concentrations of less than 0.01 M and an average percent error of 2%. Especially encouraging for the application of this technique to monitoring low solute concentrations (≤ 0.1 M in the receiver chamber during permeation experiments) was the excellent agreement at low concentration between the prepared equimolar mixture, [0.05 M methanol]:[0.05 M sodium formate], and the concentrations obtained *via* the ATR FTIR spectra analysis here, [0.052 M methanol]:[0.050 M sodium formate] using 1018 cm^{-1} and 1346 cm^{-1}, with an average overall percent error from all wavelengths of 4%.

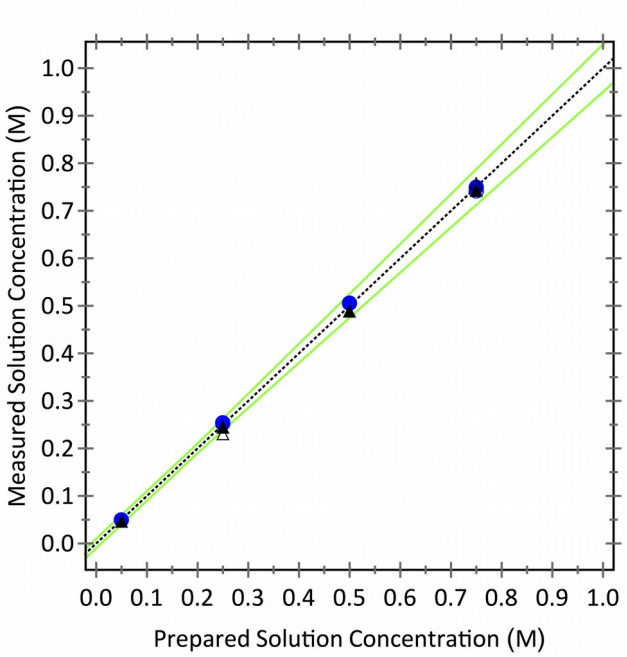

Figure S2. Concentration (M) determined via analysis of the ATR FTIR absorbance at 1018 cm^{-1} and 1346 cm^{-1} plotted against prepared solution concentration (M) for mixed solutions of (□) methanol and (□) sodium formate. Filled symbols denote equimolar solutions (*i.e.* [methanol]:[sodium formate] of [0.05 M]:[0.05 M], [0.25 M]:[0.25 M], [0.50 M]:[0.50 M], and [0.75 M]:[0.75 M]) and open symbols denote non-equimolar solutions (*i.e.* [methanol]:[sodium formate] of [0.25 M]:[0.75 M] and [0.75 M]:[0.25 M]). Dotted line denotes the identity line ($y = x$) and solid green lines denote 0.01 M or 5% deviations from the identity line ($y = x \pm 0.01$ below 0.2 M and $y = x \pm 0.05x$ above 0.2 M).

3.2 Methanol and Sodium Acetate

Results obtained for mixed solutions of methanol and sodium acetate are shown in Figure S3. The absorbances at 1018 cm^{-1} and 1413 cm^{-1} were used to calculate concentrations (see Table S5 for concentrations determined using other wavenumbers). As was the case for methanol and sodium formate, good agreement was observed between the determined and prepared solution concentrations, with an average percent error of 3.2% and average difference between actual and measured concentrations of 0.010 M. The largest relative deviations were observed for the methanol concentrations in the [0.05 M methanol]:[0.05 M sodium acetate] equimolar

mixture where the measured concentration of methanol was 0.054 M (8% error), and for the [0.25 M methanol]:[0.75 M sodium acetate] solution, where a concentration of 0.264 M was calculated (6% error). These values are fairly modest deviations in absolute terms, especially at the low methanol concentrations of interest here.

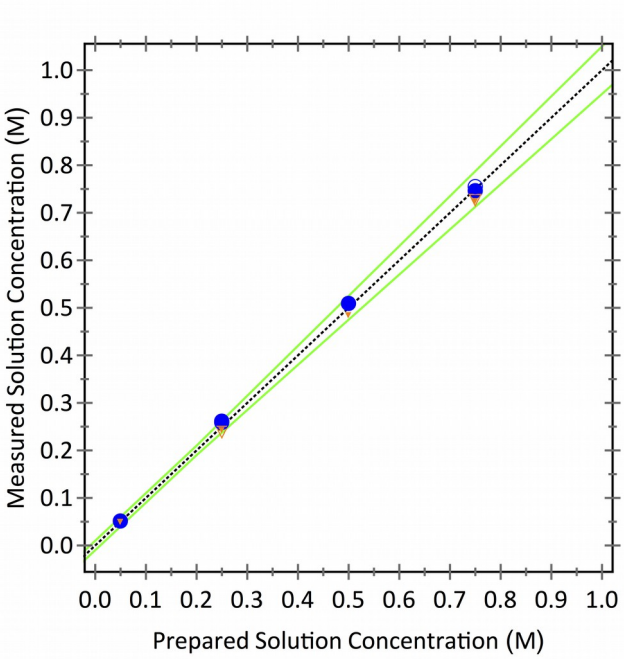

Figure S3. Concentration (M) determined via analysis of the ATR FTIR absorbance at 1018 cm^{-1} and 1413 cm^{-1} plotted against prepared solution concentration (M) for mixed solutions of (□) methanol and (□) sodium acetate. Filled symbols denote equimolar solutions (*i.e.* [methanol]:[sodium acetate] of [0.05 M]:[0.05 M], [0.25 M]:[0.25 M], [0.50 M]:[0.50 M], and [0.75 M]:[0.75 M]) and open symbols denote non-equimolar solutions (*i.e.* [methanol]:[sodium acetate] of [0.25 M]:[0.75 M] and [0.75 M]:[0.25 M]). Dotted line denotes the identity line ($y = x$) and solid green lines denote 0.01 M or 5% deviations from the identity line ($y = x \pm 0.01$ below 0.2 M and $y = x \pm 0.05x$ above 0.2 M).

3.3 Sodium Formate and Sodium Acetate

Figure S4 shows a comparison of actual concentrations of sodium formate and sodium acetate in two-solute mixed solutions with concentrations calculated using the absorbances at 1346 cm^{-1} and 1413 cm^{-1} (see Table S6 for the concentration results obtained using all ten

combinations of wavenumbers). Note the significant deviations obtained at the higher concentrations for the equimolar mixtures [0.50 M acetate]:[0.50 M formate] and [0.75 M acetate]:[0.75 M formate]. This result was characteristic of this analysis, and no combination of wavenumbers yielded satisfactory results for both sodium acetate and sodium formate above 0.25 M. Based on previous IR studies of aliphatic carboxylates, including formate and acetate, this deviation may be attributed to changes in speciation in water at higher concentrations (above *ca.* 0.3 M) [2–5]. As this concentration is well above our threshold concentration for the permeability experiments discussed in the next section (≤ 0.1 M in the receiver chamber), this phenomenon did not appreciably affect the determination of species permeabilities. In the low concentration regime of interest for permeability measurements we found excellent agreement overall. Using 1346 cm^{-1} and 1413 cm^{-1} as shown in Figure 6, [0.051 M sodium formate]:[0.053 M sodium acetate] was measured for the [0.05 M sodium formate]:[0.05 M sodium acetate] mixture (2% and 6% error, respectively).

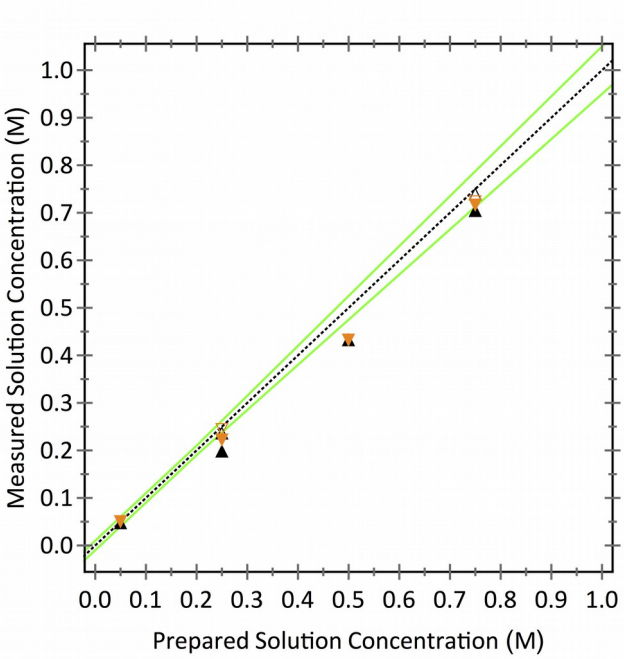

Figure S4. Concentration (M) determined via analysis of the ATR FTIR absorbance at 1346 cm^{-1} and 1413 cm^{-1} plotted against prepared solution concentration (M) for mixed solutions of (□) sodium acetate and (□) sodium formate. Filled symbols denote equimolar solutions (*i.e.* [sodium formate]:[sodium acetate] of [0.05 M]:[0.05 M], [0.25 M]:[0.25 M], [0.50 M]:[0.50 M], and [0.75 M]:[0.75 M]) and open symbols denote non-equimolar solutions (*i.e.* [sodium formate]:[sodium acetate] of [0.25 M]:[0.75 M], [0.75 M]:[0.25 M]). Dotted line denotes identity line ($y = x$) and solid green lines denote 0.02 M deviations from the identity line ($y = x \pm 0.01$ below 0.2 M and $y = x \pm 0.05x$ above 0.2 M).

3.4 Methanol, Sodium Formate, and Sodium Acetate

This analysis can also be extended to three- solute mixed solutions using Equation (7) in the main text. For mixed solutions with three solutes, the absorbance at three wavenumbers and the simultaneous solution of three equations is thereby required to determine the three unknown species concentrations. Mixed solutions of methanol, sodium formate, and sodium acetate in equimolar (0.05 M, 0.25 M, 0.50 M, and 0.75 M) and non-equimolar concentrations were prepared and analyzed. For this system the concentrations were calculated using the absorbances at 1018 cm^{-1}, 1346 cm^{-1} and 1581 cm^{-1} yielding the results shown in Figure S5 (see Table S7 for the non-equimolar mixtures). As was the case for the two-solute combinations, deconvolution of

the ATR FTIR spectra yielded quantitatively accurate solution concentrations of each component in the three-solute mixed solutions with only relatively minor deviations at high concentrations.

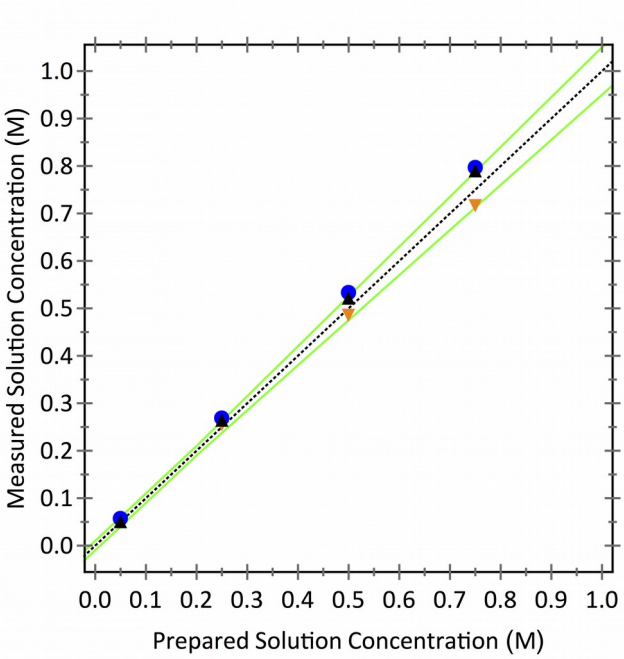

Figure S5. Concentration determined via analysis of the ATR FTIR absorbance peaks (1018 cm^{-1}, 1346 cm^{-1} and 1413 cm^{-1}) plotted against prepared solution concentration for equimolar (0.05 M, 0.25 M, 0.50 M and 0.75 M) mixed solutions of (□) methanol, (□) sodium acetate and (□) sodium formate. Dotted line denotes the identity line (y = x) and solid green lines denote 0.01 M or 5% deviations from the identity line ($y = x \pm 0.01$ below 0.2 M and $y = x \pm 0.05x$ above 0.2 M).

4. Determination of Solute Concentrations in Mixed Solutions at Other Wavenumbers

As described in the manuscript, and as employed in the previous section, the wavenumber exhibiting the greatest molar absorptivity for each solute was used to determine the concentrations of solutes in two-solute and three-solute mixed solutions. However, it is possible to determine the concentrations of methanol, sodium formate, and sodium acetate using the characteristic absorbance at several wavenumbers (Table S1). We examined the application of various wavenumbers for this purpose in addition to those noted in the main text. Additionally,

we examined how inclusion of the small or negative effective absorptivity of a species at a non-absorbing wavenumber (due to reduction in the water background) impacts the calculated concentrations. This section presents the concentrations determined using these supplemental wavenumbers and calculations.

4.1 Methanol and Sodium Formate

The solution concentrations for mixtures of methanol and sodium formate were determined using three methods. First, the contributions of methanol at 1346 cm^{-1} and sodium formate at 1018 cm^{-1} were neglected, and the concentration of methanol was calculated directly from Equation (4) using the absorbance at 1018 cm^{-1} and the concentration of sodium formate was calculated directly from Equation (4) using the absorbance at 1346 cm^{-1} (Table S4). Sodium formate exhibited essentially no absorbance at 1018 cm^{-1} (ε_{eff} = –0.0003, *c.f.* Figure 3c) with a small and negative effective molar absorptivity due to the change in the water background absorbance as sodium formate concentration increased. The molar absorptivity of methanol at 1346 cm^{-1} (ε_{eff} = 0.003859) was two orders of magnitude smaller than the molar absorptivity of sodium formate at 1346 cm^{-1} ε_{eff} = 0.149816), so it could be reasonable to neglect methanol at 1346 cm^{-1} and calculate the concentration of sodium formate directly using the absorbance at 1346 cm^{-1}. Methanol also exhibits absorption at 1115 cm^{-1} and sodium formate exhibits absorption at 1383 cm^{-1}, 1551 cm^{-1}, and 1581 cm^{-1}. However, methanol and sodium formate concentrations that were calculated using the absorbance at these other wavenumbers showed greater deviations from the actual solution concentration than did the methanol and sodium formate concentrations calculated using the absorbances at 1018 cm^{-1} and 1346 cm^{-1}, respectively These results are presented in Table S2.

Table S2: Comparison of methanol and sodium formate concentrations in binary solutions with concentrations calculated from the absorbance at various wavenumbers. Concentrations were calculated from the absorbance at the wavenumbers shown, neglecting contributions from the other solute.

Prepared Concentration (M)		**Measured Concentration (M)**						
Methanol	Sodium Formate	Methanol			Sodium Formate			
		λ [cm^{-1}] =	1018	1115	λ [cm^{-1}] =	1581	1551	1383	1346
0.75	0.75		0.752	0.811		0.740	0.707	0.793	0.765
0.50	0.50		0.508	0.541		0.511	0.476	0.539	0.505
0.25	0.25		0.255	0.312		0.268	0.247	0.281	0.254
0.05	0.05		0.052	0.057		0.056	0.051	0.059	0.051
0.75	0.25		0.744	0.817		0.243	0.218	0.305	0.253
0.25	0.75		0.256	0.439		0.755	0.753	0.788	0.768

The concentrations of methanol and sodium formate in binary solution were also calculated by neglecting the contribution of sodium formate at 1018 cm^{-1} (ε_{eff} = –0.0003) but not neglecting the contribution of methanol at 1346 cm^{-1}. The concentration of methanol calculated directly with Equation (4) using the absorbance at 1018 cm^{-1} was then inserted into Equation (5), and the measured absorbance at 1346 cm^{-1} and the effective molar absorptivities of both methanol and sodium formate at 1346 cm^{-1} were used to calculate the concentration of sodium formate. The concentrations of methanol and sodium formate so determined (Table S3) were superior to the results obtained by direct calculation of sodium formate concentration using the absorbance at 1346 cm^{-1} (Table S2), suggesting that the contribution of methanol to the absorbance at 1346 cm^{-1} was not negligible, and should be considered for most accurate concentration determination. In addition to the sodium formate concentrations calculated using the absorbance at 1346 cm^{-1}, Table S3 also shows the concentrations of sodium formate was determined using the absorbance at 1383 cm^{-1}, 1551 cm^{-1}, and 1581 cm^{-1}, including contributions

from both methanol and sodium formate at each wavenumber. The most satisfactory results were obtained using the absorbance at 1346 cm^{-1}.

Table S3: Comparison of methanol and sodium formate concentrations in binary solutions with concentrations calculated from the absorbance at various wavenumbers. The methanol concentration was calculated using the absorbance at 1018 cm^{-1}, and the sodium formate concentration was calculated from the absorbance at various wavenumbers, including contributions from methanol at those wavenumbers.

Prepared Concentration (M)		**Measured Concentration (M)**					
Methanol	Sodium Formate	Methanol	Sodium Formate				
		λ_1 = 1018 cm^{-1}	λ_2 [cm^{-1}] =	1581	1551	1383	1346
0.75	0.75	0.752		0.764	0.742	0.736	0.746
0.50	0.50	0.508		0.508	0.499	0.500	0.492
0.25	0.25	0.255		0.255	0.259	0.262	0.248
0.05	0.05	0.052		0.052	0.054	0.055	0.050
0.75	0.25	0.744		0.256	0.252	0.249	0.234
0.25	0.75	0.256		0.744	0.765	0.769	0.761

Finally, the concentrations of methanol and sodium formate were determined by accounting for the contributions of both methanol and sodium formate at two wavenumbers using a system of equations solved simultaneously for the two unknown concentrations (Equation (6)). Results are shown in Table S4 for several combinations of wavenumbers, where λ_1 = 1018 cm^{-1} or 1115 cm^{-1}, and λ_2 = 1346 cm^{-1}, 1383 cm^{-1}, 1551 cm^{-1}, or 1581 cm^{-1}. The most accurate results were obtained with the combination λ_1 = 1018 cm^{-1} and λ_2 = 1346 cm^{-1}. The results obtained using this method, where the contributions of both methanol and sodium formate were accounted for at both wavenumbers, were not more (or less) accurate than the results obtained by neglecting the contribution of sodium formate at 1018 cm^{-1}. Therefore, in calculation of concentrations during permeation experiments described later, the concentration of methanol was calculated directly with the absorbance at 1018 cm^{-1} and the contribution of sodium formate was neglected at 1018 cm^{-1}.

Table S4: Comparison of methanol and sodium formate concentrations in binary solutions with concentrations calculated from the absorbance at various wavenumbers, including the contributions of both methanol and sodium formate at two wavenumbers.

Prepared Concentration (M)		λ_1 = 1018 cm^{-1}				λ_1 = 1115 cm^{-1}			
λ_2 [cm^{-1}] =		1581	1551	1383	1346	1581	1551	1383	1346
Methanol	Sodium Formate	**Measured Methanol Concentration (M)**							
0.75	0.75	0.753	0.753	0.753	0.753	0.698	0.702	0.704	0.702
0.50	0.50	0.509	0.509	0.509	0.509	0.463	0.467	0.468	0.469
0.25	0.25	0.255	0.255	0.255	0.255	0.271	0.273	0.274	0.276
0.05	0.05	0.052	0.052	0.745	0.052	0.049	0.049	0.049	0.050
0.75	0.25	0.745	0.745	0.258	0.745	0.777	0.779	0.781	0.783
0.25	0.75	0.258	0.258	0.052	0.258	0.326	0.326	0.329	0.329
		Measured Sodium Formate Concentration (M)							
0.75	0.75	0.765	0.742	0.737	0.746	0.763	0.736	0.720	0.734
0.50	0.50	0.528	0.499	0.500	0.492	0.526	0.495	0.490	0.484
0.25	0.25	0.276	0.259	0.262	0.248	0.277	0.259	0.253	0.243
0.05	0.05	0.058	0.054	0.055	0.050	0.058	0.053	0.054	0.049
0.75	0.25	0.267	0.252	0.249	0.234	0.268	0.253	0.240	0.229
0.25	0.75	0.763	0.765	0.769	0.761	0.766	0.765	0.742	0.746

4.2 Methanol and Sodium Acetate

Analysis of solutions of methanol with sodium acetate is slightly more complex due to the overlapping absorption bands of methanol and sodium acetate around 1018 cm^{-1}. While sodium acetate had a distinct absorbance peak at 929 cm^{-1} (where methanol exhibited essentially no absorbance), the peak was relatively small and thereby less favorable for monitoring the gradual changes in solution concentration in the membrane diffusion experiments of ultimate interest here. Of additional concern at low wavenumbers was the steep slope in the water background in this region, as subtle changes over the course of a many hours in a permeation experiment can frustrate spectral analysis. Thus, for binary solutions of methanol and sodium acetate, a system of equations using the absorbance at two wavenumbers was utilized to

determine the solute concentrations. The absorbance at 1018 cm^{-1} was necessarily used (since the methanol concentration was best calculated at this wavenumber, as described previously), and the absorbance at 1346 cm^{-1}, 1383 cm^{-1}, 1413 cm^{-1}, 1551 cm^{-1}, or 1581 cm^{-1} were used to calculate the mixture concentrations using Equation (6). Results are shown in Table S5. The most accurate concentration values were obtained using the absorbance at 1413 cm^{-1}.

Table S5: Comparison of methanol and sodium acetate concentrations in binary solutions with concentrations measured from the absorbance at various wavenumbers, including the contributions of both methanol and sodium acetate at two wavenumbers.

Prepared Concentration (M)		λ_1 = 1018 cm^{-1}				
		λ_2 [cm^{-1}] = 1581	1551	1413	1383	1346
Methanol	Sodium Acetate	**Measured Sodium Acetate Concentration (M)**				
0.75	0.75	0.754	0.740	0.726	0.717	0.697
0.50	0.50	0.499	0.505	0.486	0.457	0.433
0.25	0.25	0.247	0.258	0.244	0.216	0.199
0.05	0.05	0.060	0.056	0.051	0.047	0.044
0.75	0.25	0.268	0.263	0.241	0.218	0.712
0.25	0.75	0.742	0.737	0.729	0.718	0.196
		Measured Methanol Concentration (M)				
0.75	0.75	0.743	0.746	0.749	0.752	0.756
0.50	0.50	0.508	0.507	0.512	0.518	0.524
0.25	0.25	0.263	0.260	0.264	0.270	0.274
0.05	0.05	0.051	0.052	0.054	0.055	0.055
0.75	0.25	0.750	0.752	0.757	0.762	0.768
0.25	0.75	0.258	0.259	0.261	0.264	0.265

4.3 Sodium Formate and Sodium Acetate

Determining solute concentrations in binary solutions of sodium acetate and sodium formate is analogous to the methanol/sodium acetate case, albeit more complex due to the greater number of possible combinations of useable wavenumbers: 5!/(3!2!) = 10 combinations. The concentrations for sodium formate and sodium acetate in binary solution were calculated by solving Equation (6) using the contributions of both solutes to the absorbance at two wavenumbers. Results are shown in Table S6. The concentrations of sodium formate and sodium acetate were determined most accurately using the absorbances at 1346 cm^{-1} and 1413 cm^{-1}.

Table S6: Comparison of sodium formate and sodium acetate concentrations in binary solutions with concentrations measured from absorbances at various wavenumbers, including the contributions of both methanol and sodium acetate at two wavenumbers.

Prepared Concentration (M)		λ_1 = 1551 cm^{-1}				λ_1 = 1581 cm^{-1}			λ_1 = 1413 cm^{-1}		λ_1 = 1383 cm^{-1}
	λ_2 [cm^{-1}] =	1581	1413	1383	1346	1413	1383	1346	1383	1346	1346
Sodium Acetate	Sodium Formate	**Measured Sodium Acetate Concentration (M)**									
0.75	0.75	0.718	0.724	0.672	0.662	0.724	0.855	1.607	0.72	0.719	0.625
0.5	0.5	0.443	0.434	0.455	0.445	0.453	0.406	0.406	0.435	0.435	0.407
0.25	0.25	0.237	0.221	0.274	0.264	0.222	0.125	-0.201	0.225	0.225	0.225
0.05	0.05	0.053	0.052	0.058	0.057	0.052	0.038	-0.019	0.053	0.053	0.056
0.75	0.25	0.726	0.726	0.726	0.723	0.726	0.726	0.775	0.726	0.726	0.711
0.25	0.75	0.258	0.248	0.255	0.245	0.249	0.266	0.457	0.248	0.247	0.207
		Measured Sodium Formate Concentration (M)									
0.75	0.75	0.62	0.608	0.71	0.729	0.618	0.584	0.386	0.677	0.708	0.742
0.5	0.5	0.473	0.454	0.413	0.432	0.439	0.446	0.446	0.426	0.436	0.446
0.25	0.25	0.242	0.273	0.168	0.188	0.245	0.271	0.357	0.203	0.202	0.202
0.05	0.05	0.058	0.059	0.049	0.049	0.058	0.062	0.077	0.052	0.051	0.050
0.75	0.25	0.235	0.234	0.236	0.241	0.235	0.235	0.222	0.235	0.240	0.245
0.25	0.75	0.72	0.739	0.725	0.744	0.722	0.718	0.667	0.739	0.743	0.758

4.4 Methanol, Sodium Formate, and Sodium Acetate

The concentrations of methanol, sodium formate, and sodium acetate were measured in three-solute mixed solutions. Representative concentrations obtained for equimolar and non-equimolar ternary solutions of methanol, sodium formate, and sodium acetate, calculated using the absorbances measured at 1018 cm^{-1}, 1346 cm^{-1}, and 1413 cm^{-1}, are shown in Table S7. At 1018 cm^{-1}, only the contributions of methanol and sodium acetate were included in the calculation, due to the very low effective molar absorptivity of sodium formate at 1018 cm^{-1}. At 1346 cm^{-1} and 1413 cm^{-1}, contributions from all three solutes were included.

Table S7: Comparison of methanol, sodium formate, and sodium acetate concentrations in ternary solutions with concentrations measured from absorbances at 1018 cm^{-1}, 1346 cm^{-1}, and 1413 cm^{-1}.

Prepared Concentration (M)			**Measured Concentration (M)**		
Methanol	Sodium Acetate	Sodium Formate	Methanol	Sodium Acetate	Sodium Formate
0.75	0.75	0.75	0.800	0.719	0.793
0.50	0.50	0.50	0.536	0.488	0.525
0.25	0.25	0.25	0.271	0.258	0.267
0.05	0.05	0.05	0.060	0.053	0.053
0.25	0.75	0.25	0.303	0.735	0.278
0.25	0.25	0.75	0.267	0.253	0.773
0.75	0.25	0.25	0.757	0.250	0.264
0.50	0.75	0.25	0.553	0.730	0.276
0.75	0.25	0.50	0.766	0.248	0.516
0.25	0.50	0.75	0.285	0.497	0.795

5. Apparent (uncorrected) solute diffusivities

Table S8 presents the apparent diffusivities (not corrected for the osmotic flow of water) for methanol, sodium formate, and sodium acetate. Values corrected for the osmotic flow of water through the membrane are shown in Table 4 in the main text.

Table S8. Diffusivities of methanol, sodium formate, sodium acetate, and mixtures thereof in Nafion® 117, calculated from permeabilities (Table 1) and solubilities (Table 2). For three-solute mixtures, co-solutes are: (a) sodium formate and sodium acetate, (b) methanol and sodium acetate, (c) methanol and sodium formate. Uncertainties are propagated (as described by Harris [6]) from the uncertainties reported for permeabilities and solubilities.

Apparent Solute Diffusivities (cm^2/s) in Nafion® 117			
	Methanol	**Sodium Formate**	**Sodium Acetate**
Single Solute	$(3.2 \pm 0.2) \times 10^{-6}$	$(1.3 \pm 0.1) \times 10^{-6}$	$(1.4 \pm 0.1) \times 10^{-6}$
Two-solute Mixture with Methanol	--	$(1.4 \pm 0.2) \times 10^{-6}$	$(1.5 \pm 0.3) \times 10^{-6}$
Two-solute Mixture with Sodium Formate	$(3.1 \pm 0.3) \times 10^{-6}$	--	$(1.7 \pm 0.2) \times 10^{-6}$
Two-solute Mixture with Sodium Acetate	$(3.0 \pm 0.3) \times 10^{-6}$	$(1.5 \pm 0.1) \times 10^{-6}$	--
Three-solute Mixture	$(2.4 \pm 0.2) \times 10^{-6(a)}$	$(1.6 \pm 0.6) \times 10^{-6(b)}$	$(1.3 \pm 0.6) \times 10^{-6(c)}$

References

[1] B.M. Carter, B.M. Dobyns, B.S. Beckingham, D.J. Miller, Multicomponent transport of alcohols in an anion exchange membrane measured by *in situ* ATR FTIR spectroscopy, Polymer. 123 (2017) 144–152. doi:10.1016/j.polymer.2017.06.070.

[2] F. Génin, F. Quilès, A. Burneau, Infrared and Raman spectroscopic study of carboxylic acids in heavy water, Phys. Chem. Chem. Phys. 3 (2001) 932–942. doi:10.1039/b008897h.

[3] J. Čeponkus, D. Leščiūtė, D. Čepulinskaitė, M. Pučetaitė, V. Šablinskas, Association of water and small monocarboxylic acids: Matrix isolation FTIR spectrometry study, Lith. J. Phys. 49 (2009) 53–62. doi:10.3952/lithjphys.49102.

[4] J.E. Tackett, FT-IR Characterization of Metal Acetates in Aqueous Solution, Appl. Spectrosc. 43 (1989) 483–489. doi:10.1366/0003702894202931.

[5] I.A. Heisler, K. Mazur, S. Yamaguchi, K. Tominaga, S.R. Meech, Measuring acetic acid dimer modes by ultrafast time-domain Raman spectroscopy., Phys. Chem. Chem. Phys. 13 (2011) 15573–9. doi:10.1039/c1cp20990f.

[6] D.C. Harris, Quantitative Chemical Analysis, Sixth Edit, W. H. Freeman and Company, New York, 2003.